Focal Point



November 2026 • Volume X • Issue 2

Focal Point, *noun*
1. A point of convergence of a beam of particles
2. A state or condition permitting clear perception or understanding
3. A center of activity, attraction, or attention

Cover image taken in August 2025 by *Yong Ding '27*

No copyright infringement is intended at any point, and effort was made to credit works appropriately. However, if you find some mistake in our accreditation of works, please contact us.

This issue of Focal Point was printed at Deerfield Academy.
7 Boyden Lane
Deerfield MA 01342

Focal Point is a non-profit magazine created by students of Deerfield Academy, with the support from our faculty advisor, Dr. Mark Acton.

DEERFIELD ACADEMY

Focal Point

Volume X

Issue 2

November 2026

November 2026 • Volume X • Issue 2

Contents

The Sciences

1 • A New Look Into the Past: The Newest NASA Telescope, Nancy Grace Roman • *Gabby Kilroy ’29*

3 • Are Boltzmann Brains Real? • *Angela Han ’29*

5 • Effectiveness and Safety of rVSV-ZEBOV Vaccine Against Zaire Ebola Virus • *Jerry Du ’27*

8 • Exoplanets: A World Outside of Our Own • *Elise Mehfar ’29*

10 • The Types of Prion Diseases • *Akari Higashida ’28*

11 • An Overview of CRISPR • *Russell Fan ’28*

Technology

12 • Origin of Life: Spontaneous Proliferation? • *Krystal Zhang ’29*

14 • HistGramBench: Can AI Pass Mr. Dollhopf’s Geometry Class? • *Harry Tran ’28*

18 • Bacteria as Living Circuit Boards • *Millie Huang ’29*

20 • Quantifying Error in Harmonic Reduction Systems • *Carter He ’28*

24 • Why Starship? • *Ted Huang ’29*

History

25 • How City Design Shaped the Spread of Disease in Europe and the Pre-Columbian Americas • *Allan Kang ’29*

26 • Why do we care about our bodies after we die? • *Leo Feng ’29*

A New Look Into the Past: The Newest NASA Telescope, Nancy Grace Roman

GABBY KILROY '29

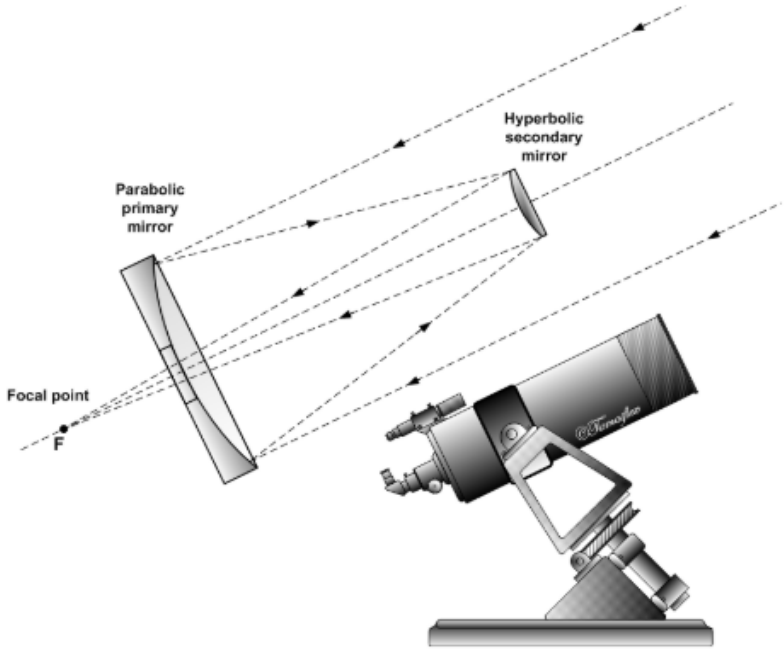
On August 30, 2026, National Aeronautics and Space Administration (NASA) launched its newest space telescope, the Nancy Grace Roman Space Telescope (Roman), named after NASA's first Chief of Astronomy, Nancy Grace Roman. It is currently heading towards an orbit 930,000 miles (1.5 million kilometers) away from Earth, in the gravitational "sweet spot" known as the second Sun-Earth LaGrange point.

In 1959, Nancy Roman joined the agency, first woman to hold an executive position at the company. She played a pivotal role in turning the company from a small organization to one of the most famous space agencies in the world. Despite receiving backlash and discouragement from her mentors and peer scientists, Roman successfully lobbied Congress to approve funding for the creation of the Hubble Space Telescope. Her contributions led NASA to create a space telescope in her name, leading us to the present day launch of the Nancy Grace Roman Space Telescope.

The concept of a new telescope was recommended in the 2010 Astronomy and Astrophysics Decadal Survey. Six years later, NASA began the process of formally beginning the development process of Roman. Six years after that, it was finally launched from NASA's Kennedy Space Center in Florida. Roman is not merely another telescope; it has an intended purpose of surveying wide-fields of space at high resolution putting it on the same level (if not higher) than Hubble or James Webb Space Telescope (JWST).

The origins of Roman are a fascinating representation of the reusability of technology. The National Reconnaissance Office (NRO), which built spy equipment for agencies such as the CIA, also built the optical mirrors necessary for telescopes to observe aspects of the universe. In 1999, the NRO started a multi-billion dollar program called "Future Imaginary Architecture" (FIA) which aimed to design spy satellites to surveil people and Earth from above. The NRO hired Boeing to create the technology. After the attacks of 9/11, the US federal government dumped even more money into the project under stress of foreign invaders and spies. However, delays and budget issues caused the program to fail, wasting billions of dollars. In 2005, the *New York Times* deemed the project, "perhaps the most spectacular and expensive failure in the 50-year history of American spy satellite projects." Fortunately, the FIA gifted NASA two 2.4 meter mirrors in 2012 that were used in the satellites. According to Space.com, "[the] optics [were] said to be similar to the Hubble Space Telescope's." Even though NASA originally approached the donation with skepticism, as the Roman had only recently been proposed, an agreement of the majority in the 2010 National Academy of Science Astronomy and Astrophysics Decadal Survey showed Roman to be the top priority for completion in the world of science. The rejected mirrors were subsequently repurposed into crucial pieces for the optical function of the telescope.

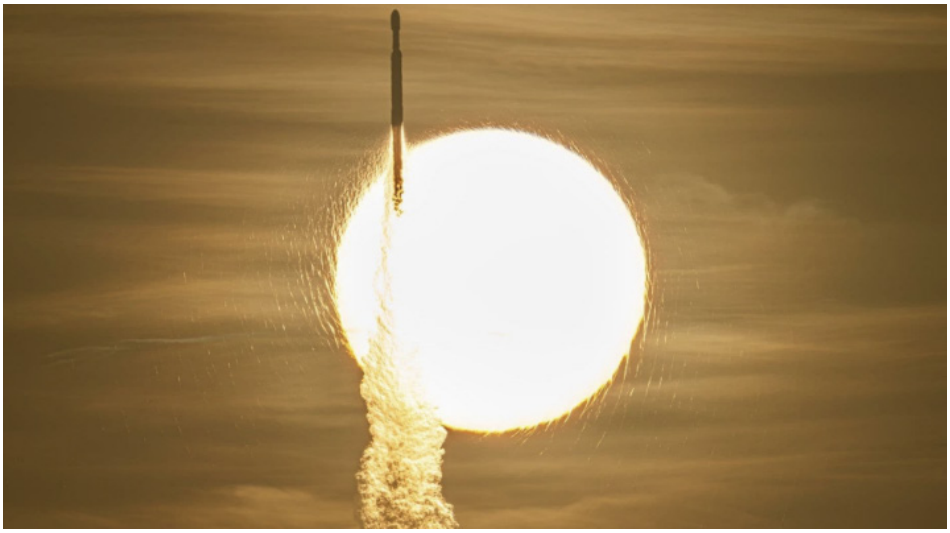
In addition to the 2.4m primary mirrors, the telescope also includes secondary mirrors, chronograph instruments, a wide-field instrument, and an outside metal shell that protects the inside technology. As described by Gunter's Space Page, the wide-field instrument has two channels, "a wide field channel and an integral field unit (IFU) spectrograph channel." The wide-field channel is comprised of three mirrors and a grism wheel, which is a rotating disk used in astronomical telescopes that has the ability to slide different optical filters into the light path, allowing space and ground telescopes to switch between simple imaging and low/medium resolution slitless spectroscopy (view diagram above). Although a rather convoluted structure, the telescope has the ability to take images in infrared, a type of light



SZŐCS TAMÁS (TAMASFLEX)/WIKIMEDIA COMMONS, CC BY-SA 3.0 [14]

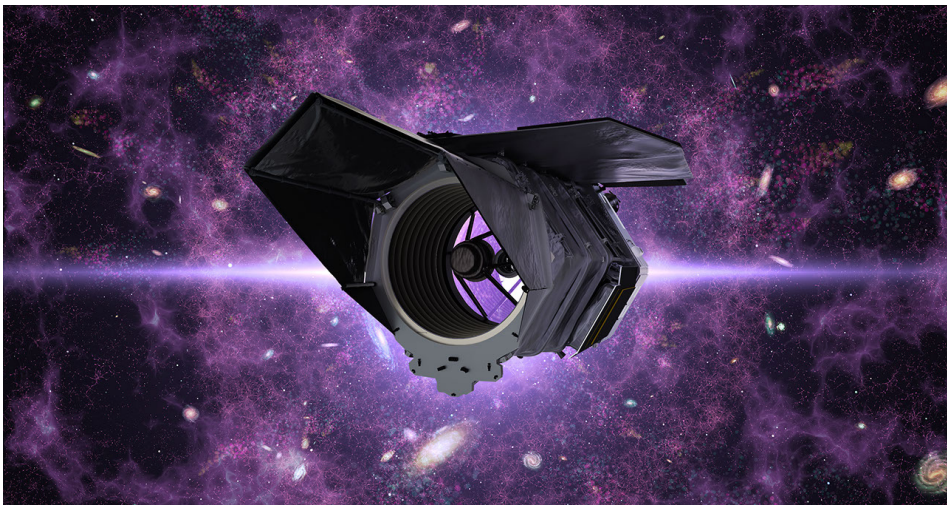
with wave length longer than about 750nm that humans can't see. Roman, along with other telescopes such as the James Webb Space Telescope, uses spectrographs to convert infrared heat into visible light. The IFU channel uses an image slicer and spectrograph to provide, "individual spectra of each 0.15 wide slice covering the 0.6 — 2.0 μm spectral range over a 3.00 × 3.15 arcsec field." (Gunter's Space Page) Thus, the IFU channel has the ability to give researchers the individual spectra of each part of the large image, allowing the utmost specificity and in-detail images of any part of the universe. Not only did the development of the Roman represent a significant step forward in NASA's aeronautical engineering, but the telescope's launch will also catapult our knowledge of outer space through its improved technology.

According to Gunter's Space Page, "The wide field instrument provides the wide-field imaging and slitless spectroscopic capabilities required to perform the Dark Energy, Exoplanet Microlensing, and NIR surveys while the coronagraph instrument supports the Exoplanet high contrast imaging and spectroscopic science." Dark energy is the hypothesized form of energy that drives the expansion of the universe. Roman can track thousands of supernovae, and through measuring the brightness of the supernovae and how much their light bends, it can also track how the universe's expansion changes as time passes, subsequently adding to the knowledge of dark energy. Roman's wide view assists the study of exoplanets in three different ways: gravitational microlensing, transit detection and direct imaging. Gravitational lensing is a method of determining a planet's mass and its distance from a host star by analyzing the distortions of space-time created by a star's gravity when a planet passes by the star. This ripple is quantifiable, allowing astronomers to locate exoplanets on an enlarged scale. Transit detection—the way that most exoplanets have been discovered—is the measurement of when a planet passes by a star while it's orbiting and momentarily blocks the light of the star, signaling to researchers that a planet is orbiting that star. Since exoplanets are miniscule compared to the stars they orbit and the light those host-stars emit, direct imaging has always been difficult as researchers often can't record a large enough blockage of light to pinpoint an exoplanet. Additionally, despite the difficulty of acquiring images of exoplanets, Roman's combination of ultra precise data capturing and wide scope enables the discovery of exoplanets through direct imaging on another level. Now, telescopes can take pictures of actual exoplanets and conduct direct research from the image. Roman's placement also plays a significant role in its ability to capture clear images of the universe from a point close to Earth. Facing away from the sun, it blocks out any solar light, only collecting data from an unobstructed viewpoint.



JOHN KRAUS/NASA [16]

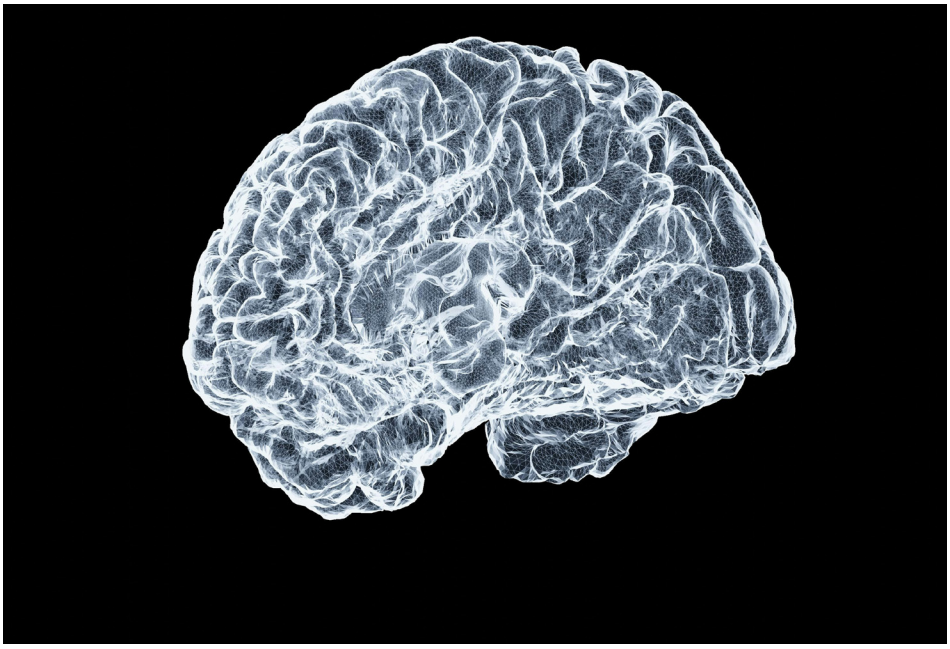
The Roman telescope doesn't just give the scientific community cool pictures of nearby nebulae or stars, it enables the discovery of new earth-like exoplanets and provides more information about the elusive existence of black energy. From a failed spy satellite mirror to the newest scientific advancement launched into space able to capture 100x that of the Hubble space telescope, the Nancy Grace Roman Space Telescope is the next look into the universe and the worlds beyond our own.



NASA'S GODDARD SPACE FLIGHT CENTER [15]

Are Boltzmann Brains Real?

ANGELA HAN '29



SHAWN DAY/UNSPLASH [6]

Consider the following: a lone brain, suspended in an interminable stretch of the cosmos. It contains memories of what seems like a lifetime, hopes, and dreams, only to disintegrate into chaos a split second later. According to thermodynamics, you are more likely to be such a brain than not.

How can that possibly be?

Entropy may offer an answer. First conceived by Rudolf Clausius in his 1850 paper "On the Moving Force of Heat," entropy describes how spread out or unavailable energy is within a physical system [1]. Clausius and other scientists in the then-nascent field of thermodynamics postulated that the overall entropy of an isolated system will increase and tend towards a maximum—what would become known as the second law of thermodynamics.

Initially, physicists believed that the increase in entropy in an isolated system was absolute. Imagine a hot metal bar pressed against a cold one. Wait long enough, and the system transitions towards thermal equilibrium, evolving from a low-entropy state with a steep temperature gradient to a high-entropy configuration where heat is evenly distributed. This makes intuitive sense. Everything tends towards a state of equilibrium. Heat only flows from hot to cold, never the other way around. Or does it?

In reality, this could happen—it's just unlikely. In the 1870s, physicist Ludwig Boltzmann proposed a statistical interpretation of entropy:

$$S = k_B \ln W,$$

where S represents the total entropy of a system, k_B is Boltzmann's constant (1.38×10^{-23} m^2 kg/(s^2 K)), and W is the total number of possible microscopic arrangements (microstates) of the system [1]. This equation reformulates entropy in terms of probability. Imagine the two metal bars again. If heat is regarded as discrete energy packets randomly exchanging between particles, an exchange that temporarily decreases the cold bar's energy is possible, however unlikely. This is the core of Boltzmann's great insight: the universe is ruled not by certainty, but by overwhelming probability.

This new interpretation of entropy gives rise to interesting results, especially when applied to the universe, the only true closed system in existence. Back in 1862, Lord Kelvin first envisioned a future where all energy would be spread so thin that nothing could stir. Provided that the laws of thermodynamics remained constant in the future, he reasoned, everything would inevitably enter "a state of universal rest and death" [5]. This picture, known as the heat death of the universe, is a widely accepted theory of the fate of our universe. However, though the universe may seem "dead" on a global scale, the statistical interpretation of the second law of thermodynamics suggests that it is possible for a local reversal of entropy to occur.

One such possibility is the Boltzmann brain: a self-aware entity born from spontaneous fluctuations after the heat death of the universe. It is difficult for these structures to form. After reaching heat death, the most common particles in the universe will be photons and gravitons, which typically possess extremely low energy. However, it is rare but still possible for high-energy photons and gravitons to appear and collide with each other, leading to the creation of fermion particle-antiparticle pairs. While nearly all such pairs almost instantly annihilate each other, some of these particles can, in theory, travel far enough from each other to encounter other matter. In the extremely unlikely case that enough matter was produced and retained this way, more complex macrostructures like brains could form.[3]

Despite their unlikelihood, Boltzmann brains are expected to vastly outnumber ordinary observers. In fact, it is more likely for a single mind to arise by accident than for a vast, orderly universe to painstakingly evolve over billions of years. First, assembling a brain complete with illusory memories requires exponentially less entropy reduction than assembling an entire universe containing billions of galaxies, planets, and evolving biospheres. Furthermore, given an infinite amount of time after heat death, however unlike they are, Boltzmann brains are guaranteed to form an infinite number of times. So, by the decrees of modern scientific theory, our treasured reality could be nothing more than a hallucination afloat on a statistical sea of infinite brains.

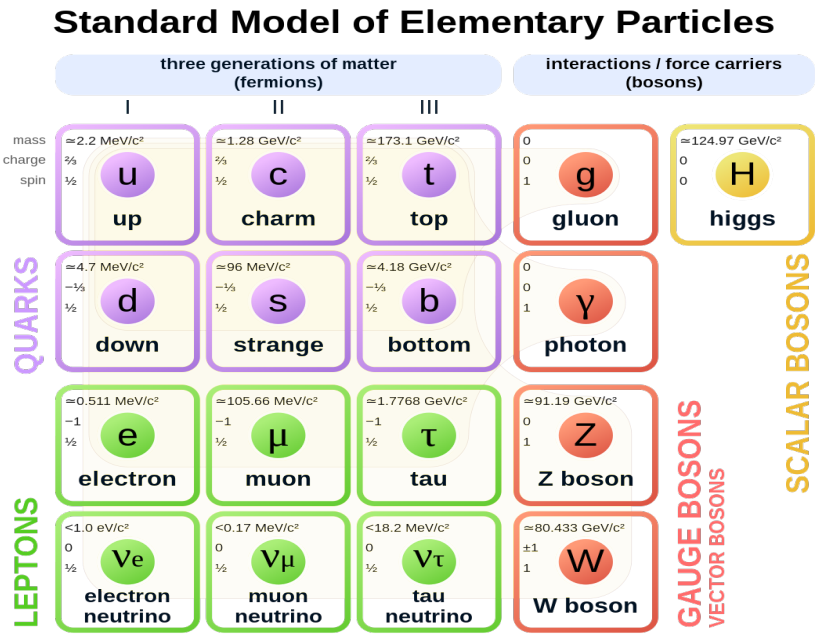
That's absurd, you may think. You have a physical body and memories. You can't

be a Boltzmann brain, can you? Unfortunately, there's no way to definitively rule out the possibility that you are such a brain. After all, the sensory evidence of the world around you could just be arbitrary illusions. Yet there's a twist: by the same logic, it is impossible to reasonably show that you are a Boltzmann brain. This is what physicist Sean Carroll calls "cognitively unstable": if you accept that you are a Boltzmann brain, you would have to reject the validity of your own cognitive faculties, observations, and memory—the fundamental assumption upon which all scientific theories, including the Boltzmann brain argument itself, are founded [3]. The Boltzmann brain is therefore considered a theory that, if shown to be true or overwhelmingly likely, signifies a latent error in our current understanding of the universe—known as a reductio ad absurdum. What could we have gotten wrong?

In 2013, Carroll and fellow physicist Kimberly Boddy came up with the idea that the universe simply may not exist long enough to reach heat death. The properties and interactions of all matter in the universe are determined by quantum fields. Most fields are in the lowest energy level possible—a state known as the vacuum state [2]. However, measurements of the Higgs boson showed that the Higgs field, which gives mass to matter, may not be in its vacuum state. That is, a lower energy "true vacuum" may exist for the Higgs field. In the case of a random event like quantum tunneling, the Higgs field could bypass the potential energy barrier between its current metastable state and its true vacuum state. This would trigger the formation of a spatial bubble of the true vacuum state that expands at the speed of light and, for all we know, could completely change the laws of particle physics as we know them—and with them, the possibility of the random fluctuations that lead to Boltzmann brains. If this event, known as false vacuum decay, is more likely to occur before heat death, the expected number of Boltzmann brains would be drastically reduced. Yet, later studies show that this may not be the case. The amount of time before false vacuum decay occurs depends on more specific measurements of elementary particle masses, which reflect the stability of the Higgs field. Boddy and Carroll calculated that a top quark pole mass of around 178 GeV is indicative of a decay rate that could prevent the universe from reaching heat death [2]. However, more recent measurements place the quark's mass at around 172.93 ± 1.36 GeV, suggesting a far stabler Higgs field and a lower decay rate [4].



UNKNOWN PHOTOGRAPHER (1902)/WIKIMEDIA COMMONS [7]



NEW WORLD ENCYCLOPEDIA [8]

At any rate, we are a long way off from establishing a cosmological model that steers clear from the implication that our perception of reality is a mere low-entropy, near-instantaneous fluctuation in a dead universe. However, because the Boltzmann brain scenario is cognitively self-undermining, scientists are rationally entitled to reject it. Though the theory cannot be empirically disproven, cognitive stability demands that we trust our observations before a new model of the universe eliminates the statistical dominance of Boltzmann brains for good.

Effectiveness and Safety of rVSV-ZEBOV Vaccine Against Zaire Ebola Virus

JERRY DU '27

Introduction

Ebola virus (EBOV) is a member of the Filoviridae family. First identified in the 1976 outbreaks of Sudan and the Democratic Republic of the Congo, the virus earned its name from the Ebola River. EBOV causes hemorrhagic fevers that often lead to death. EBOV's rapid transmission and significant public health implications causes sporadic outbreaks with high mortality rates particularly in sub-Saharan Africa [1]. Ebola virus disease (EVD) is due to the infection by one of the Ebola virus species, the most lethal being the Zaire Ebola Virus (ZEBOV). This virus is transmitted to humans through contact with infected animals, such as fruit bats, and transmitted among humans by direct or indirect contact with the bodily fluids. Symptoms include sudden onsets of fever, weakness, muscle pain, and, in severe cases, internal and external bleedings [2]. The 2013-2016 outbreak of ZEBOV in West Africa, the largest EBOV outbreak up to date, resulted in more than 28600 reported cases of EVD and 11325 deaths [3]. The epidemic emphasized the lack of disease surveillance, preparation and treatment. Since then, significant effort in the medical field has guided us to have a more detailed understanding of the virus.

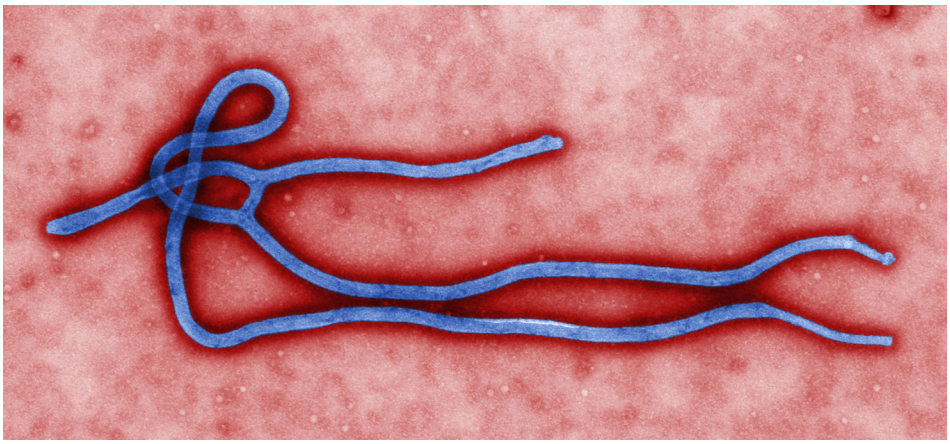
The invention of a vaccine against ZEBOV would be vital to combat and prepare for future epidemics. Early efforts to develop Ebola vaccines date back to the 1990s and early 2000s, but these were often limited to preclinical stages due to challenges including biosafety concerns, limited funding, and sporadic outbreak patterns that hindered large-scale trials [4]. Initial vaccine candidates included a variety of different approaches, such as DNA-based vaccines, adenovirus-vectored approaches, and virus-like particles. Although some did show promise in animal testing, none progressed to the final stages of clinical trial [5]. Later in the process, the West Africa epidemic impelled international cooperation and the acceleration of vaccine development.

The most notable outcome of the efforts was the invention of the rVSVΔG-ZEBOV-GP. This vaccine demonstrated high efficacy in a landmark ring vaccination trial conducted in Guinea in 2015, which showed near-complete protection among vaccinated individuals. Following further clinical evaluation, the vaccine received approval from both the World Health Organization (WHO) and the U.S. Food and Drug Administration in 2019, becoming the first licensed vaccine for EVD [6]. In addition, other vaccines such as ChAd3-EBO-Z/S, Ad26.ZEBOV/MVA-BN-Filo and multivalent or pan-ebolavirus vaccines are in experimental trials and have all revealed promising results [6].

This literature review investigates the pre-existing trials conducted using the rVSVΔG-ZEBOV-GP vaccine. By reporting and comparing methods, data, and conclusions from previous studies, this paper will provide a review of the immunogenicity, the ability for the vaccine to trigger immune responses, and adverse events (AE), any harmful medical occurrence during clinical trials. The purpose of this paper is to understand the effectiveness and safety of the vaccine.

Vaccine Mechanism and Function

The recombinant vesicular stomatitis virus–ZEBOV envelope glycoprotein vaccine (rVSVΔG-ZEBOV-GP) is the most effective and applied vaccine against EBOV. The vaccine, commercially known as Ervebo, is a recombinant, replication-competent viral vector vaccine designed to offer protection against ZEBOV. Recombinant vaccines, like the Ervebo, are made by using a gene of EBOV and adding it to the vesicular stomatitis virus. This vaccine, originally developed by the Public Health Agency of Canada, uses rVSV, Indiana Strain, as a vector to provoke an immune response against ZEBOV by replacing the gene encoding vesicular stomatitis virus (VSV) surface glycoprotein (G protein) with the gene encoding ZEBOV GP [6]. Following intramuscular injection, the vaccine virus enters host cells via endocytosis. The vaccine utilizes the Ebola GP to bind to host cell receptors and mimics natural Ebola virus entry. Then, the recombinant VSV replicates locally at the injection site and in regional lymph nodes, expressing the Ebola virus GP on its surface during replication. As a result, adaptive immune responses occur [7]. rVSVΔG-ZEBOV-GP vaccine may induce adverse events including pain and oedema at the injection site and fever, chills, fatigue,



Colorized transmission electron micrograph of an Ebola virus virion.

CYNTHIA GOLDSMITH/CDC, PUBLIC DOMAIN [15]

headache, myalgia, arthralgia, lymphopenia and arthritis, all of which are transient and of mild to moderate intensity [6].

Effectiveness of the Vaccine

Over the last decade, rVSVΔG-ZEBOV-GP has stepped into Phase I and Phase II testing, presenting relatively satisfactory results through multiple clinical trials with diverse methodological approaches.

Phase III randomized, double-blind, placebo-controlled studies, like the one conducted by Halperin et al [7]. proved the vaccine's immunogenicity by measuring ZEBOV-GP-specific antibody responses via enzyme-linked immunosorbent assay (ELISA) and plaque reduction neutralization tests (PRNT). These assays demonstrated a >58-fold increase in geometric mean titers (GMTs) by day 28, with sustained responses over 24 months, confirming long-term immune memory. Over 94% of recipients seroconverted by day 28, and ≥91% maintained immune responses at 24 months. Antibodies also peaked at 18 months and remained elevated. The design of the study, using consistent testing and stratified sample groups, presented itself with strong validity. Its large sample size (N=1,197) was proven to be relatively representative of a healthy adult population.

Pediatric studies, such as the phase II trial by Alabi et al [8]. expanded the evidence base by assessing immunogenicity in children aged 1–12 years. A randomized, controlled, open-label design, the trial measured ZEBOV-GP IgG responses and neutralizing antibody kinetics over 12 months. Results showed seroconversion rates of 87–97% by day 28. Antibody titers persisted for 12 months, and neutralization functions peaked early and remained stable.

The immunogenicity in individuals with pre-existing immunity was studied in Guinea. This study discovered that 16.3% (228/1403) of participants had baseline anti-GP IgG antibodies, possibly from pre-exposure [9]. After vaccination, 81.3% (955/1175) of seronegative individuals seroconverted, while those with baseline antibodies saw a significant rise in GMTs (0.237 IU/mL vs. 0.106 IU/mL in seronegative participants, $p < 0.0001$). These results show that the rVSVAG-ZEBOV-GP effectively boosts immunity regardless of prior exposure. This finding was extremely critical since the pre-existing immunity characteristic applied to outbreak settings [9]. Thus this study supports the vaccine's utility in boosting immune responses across populations.

Given that the populations and sample groups varied in sizes and traits, the studies could not empirically provide any justification of an overall cost-benefit analysis of the virus. However, based on the lab results from the studies above, the immunogenicity of the rVSVAG-ZEBOV-GP vaccine was well tested and empirically supported with different sample groups. The rVSVAG-ZEBOV-GP vaccine is highly effective in preventing EVD through rapid protection in outbreak settings and robust immunogenicity in diverse populations.

Safety of the Vaccine

The safety profile of the rVSVAG-ZEBOV-GP vaccine was evaluated under an extensive number of studies with various methods and different populations, such as adults, children, and high-risk frontline workers, etc. Overall, clinical trials consistently report that the vaccine is relatively well-tolerated with the AEs primarily being mild to moderate and transient.

In a phase II study of adults receiving a delayed booster at 18 months, reactogenicity post-booster was comparable to primary vaccination, with no new safety signals [10]. The sample group of the trial were individuals who received primary vaccination with 2×10^7 plaque-forming units per mL of VSVΔG-ZEBOV-GP and received a booster, same with the previous vaccine, after 18 months [10]. In terms of safety, previously documented AE, arthritis, occurred in 9% of primary vaccines but did not recur post-booster. Serious adverse events (SAEs), such as epistaxis and gastrointestinal hemorrhage, were rare and not related to the vaccination. All the results show that the homologous boosting vaccines do not increase nor exacerbate AEs. Halperin et al.'s Phase 3 Trial evaluated safety in healthy adults [7]. This randomized controlled trial involved 1,197 healthy adults and found that the vaccine was generally well tolerated. Participants received one lot of rVSVΔG-ZEBOV-GP (standard dose: 2×10^7 plaque-forming units [pfu]), a high-dose formulation (1×10^8 pfu), or placebo. The study revealed relatively mild AEs, including injection-site pain (58.8% vaccinated vs. 21.8% placebo) and systemic AEs like fatigue (49% vs. 28%) [7]. SAEs were rare and not vaccine-related, with no deaths corresponding to the vaccine. Interestingly, female sex and prior arthritis history were identified as potential risk factors for post-vaccination arthritis, though severe cases were uncommon [7].

The vaccine has been tested in live scenarios against EBV. Applying this vaccine in a frontliner setting against the virus can prove how the safety was demonstrated in a dangerous environment. A study of 2,016 vaccinated frontline workers in Guinea surveillance, with structured diaries for AEs [11]. The use of control groups of unvaccinated population allowed for comparative assessment of AE frequencies with Fisher's exact. Results indicate that over 70% reported at least one AE within the first three days post-vaccination, with the most common symptoms being headache (52%), fatigue (46%), arthralgia (25%), and subjective fever (24%) [11]. Fever, a concern in Ebola-endemic regions due to the overlap of symptoms with EVD, was reported in 15% of participants, and most cases were low-grade (<39°C) and resolved within 48 hours. These findings were consistent with phase 1 trials, showing that the vaccine's AEs are manageable and self-limiting.

The vaccine's effectiveness with populations closely in contact with EVD is extremely essential, as this would be the primary population vaccinated in the future. Watson et al. studied vaccinated close contacts of EVD survivors, which included individuals with pre-existing immunity. The study found no significant difference in AE rates between seropositive and seronegative participants, with headache (35.1%), fatigue (23.7%), and muscle pain (14.6%) as the most common reactions [9]. There were only eight moderate and one severe adverse event reported, none of which were attributed to vaccination. This study provided critical evidence that pre-existing immunity does not worsen reactogenicity, thus making the vaccine suitable for environments with pre-existing exposure to EVD. Davis et al. conducted an observational follow-up study of 26 vaccinated individuals in the UK, a cohort design with standardized adverse event reporting over 12 months [12]. The study ex-

amined vaccination following exposure to a healthcare worker with Ebola virus disease (EVD) reactivation. Results showed that the vaccine was well tolerated, with no severe AEs reported [12]. Common AEs included fatigue (81%), headache (69%), myalgia (69%), and fever (50%), all of which were transient and resolved without much intervention. Throughout the trial, 50% of participants developed a fever ≥37.5 °C [12]. Two cases of arthralgia were observed but were unrelated to vaccination after review. This evidence suggests that although AEs are common, the vaccine remains safe for emergency use [12].

Systematic reviews and network meta-analyses compared the safety of multiple Ebola vaccines, including rVSV-ZEBOV. Diallo et al. used models to estimate odds ratios for AEs, with P-scores to rank vaccine safety profiles [13]. The analysis confirmed that rVSV-ZEBOV has a higher chance of injection-site pain (P-score 0.90 for lower doses) and AEs such as fatigue and headache compared to other candidates. However, these AEs were mainly mild to moderate, with severe events being rare [13]. The study claimed the vaccine's AEs were dose-dependent, with higher doses (e.g., 2×10^7 PFU) associated with increased but manageable side effects. There were no anaphylaxis or life-threatening reactions reported, further demonstrating the vaccine's safety [13].

Discussion

The primary intent of this paper is to analyze different results of the safety and effectiveness of the rVSVΔG-ZEBOV-GP vaccine. It demonstrated high immunogenicity and strong safety profile as a vaccine to prevent EVD caused by ZEBOV. Clinical trials in diverse populations, including adults, children, individuals with pre-existing immunity showed strong efficacy. Seroconversion rates, which is the production of antibodies in the blood of a person, a valuable way for studies to measure effectiveness, exceeded 90% in most studies, with durable antibody responses lasting up to 24 months, which then indicates the long-term reliability of this vaccine.

The vaccine's mechanism, utilizing a recombinant VSV vector to express ZEBOV glycoprotein, is very effective in generating immune responses. Watson et al [9]. explained the mechanism and demonstrated that the vaccine effectively boosts immunity even in individuals with pre-existing antibodies, with individuals showing an 81.3% seroconversion rate. This finding is particularly useful in settings where reoccurring can occur. The rapid protection offered, typically within 10 days as observed, makes this vaccine very valuable for epidemic control.

In addition, the vaccine's safety profile is very strong and secure. Vaccination only leads to transient mild to moderate AEs, which are all very manageable. Common AEs are injection-site pain, fatigue, headache, and low-grade fever. They were frequently reported but never escalated to a life-threatening level. In most safety trials, there was an absence of SAEs. These AEs were very acceptable as trade-offs given its high immunogenicity and efficacy. Overall, the benefits of vaccination outweighed the harms, especially in high-exposure environments. Davey et al. found that adverse events after booster vaccination were like primary vaccination [10]. Common reactions such as injection-site pain, fatigue, and headache were generally mild to moderate, as reported by Juan-Giner et al [11].

Although the vaccine is effective and safe, several limitations in current research exist. One critical limitation is the lack of long-term data over 24 months, as explained by Halperin et al., whose Phase 3 trial showed sustained antibody responses but did not extend follow-up further [7]. Indeed, studies confirm durable immunity for up to two years, but the duration of protection in endemic regions needs further research. Moreover, the current trials lack research on individuals with weak or failing immune systems, such as those with HIV. Watson et al. researched pre-existing immunity but did not address people with immune deficiency [9]. This leaves a gap of understanding in high-risk populations.

Furthermore, the vaccine induces fever, which is a symptom overlapping with EVD. This poses challenges in outbreak settings, presented in the study by Juan-Giner et al [11]. There is a need for post-vaccination monitoring to distinguish vaccine-related AEs from actual EVD infection.

The rVSVΔG-ZEBOV-GP vaccine has already given people the opportunities to react to Ebola outbreak response, but its future applications are beyond emergency use. Combining this vaccine with other candidates and vaccines could enhance cross-protection against multiple species of the virus. This can solve the problem of the lack of a "pan-EBOV vaccine".

This vaccine's efficiency is also great for global health security. Future research should explore its use as a mechanism for other hemorrhagic fever viruses, such as Marburg or Lassa virus. This approach could fasten vaccine development for emerging infectious diseases, as suggested by Diallo et al. in their comparative analysis of Ebola vaccine platforms [13].

Conclusion

The rVSVΔG-ZEBOV-GP vaccine has proven to be a great tool in Ebola prevention. Its strong efficacy and an acceptable safety profile across diverse populations can greatly benefit the current system. Its rapid and durable immune responses can also serve as a great solution for high-risk settings. The vaccine is a landmark in global health preparedness, offering a powerful defense power against future outbreaks. The innovation in vaccine deployment and combination strategies will further strengthen how humankind can combat Ebola and related emerging infectious diseases.

Exoplanets: A World Outside of Our Own

ELISE MEHFAR '29

Over 6,000 exoplanets have been discovered in the three decades since the first planet was discovered outside our solar system. NASA's definition of an exoplanet is "any planet outside of our solar system." As our space knowledge increases and our telescopes improve, the number of discovered exoplanets will continue to rise.

The first discovery of an exoplanet came in 1992 at the Arecibo Observatory in Puerto Rico, when two exoplanets were discovered orbiting PSR B127+12, a pulsar 2,300 light years away from Earth: Poltergeist (PSR B1257+12 c), with a distance of 34 million miles from the pulsar, and Phoebeter (PSR B1257+12 d), with a distance of 43 million miles. In 1994, a third planet, Draugr, was discovered in the same system 17.4 million miles from the pulsar star. These first exoplanet discoveries were groundbreaking in the field of astronomy and led to the discoveries of other celestial objects, ultimately revolutionizing our understanding of our universe.

How do exoplanets take form? It all begins in a nebula, or a cloud of gas and dust, where once disturbed by a celestial object, the matter is pulled toward the center, which will later go on to form the host star. When the cloud begins to shrink, the matter starts spinning in a disk-like shape and flattens. Once this happens, the small particles of gas and dust run into each other and stick together, forming pebbles and eventually larger rocks. As the rocks crash into each other, their gravity increases, allowing them to collect other parts of debris. The rocks grow larger and larger as the host star forms. Once the rocks (now planetary embryos) become large enough, they can clear their own orbit. Once the clearing occurs, they are officially considered planets.

While there are many ways of categorizing exoplanets, the broader categories include terrestrial, neptunians, super-Earths, and gas giants. Terrestrial planets are small planets primarily composed of rock, metal, silicate, and carbon, with a solid or liquid surface. Some may have atmospheres of liquid water, such as LHS 1140 b, whose density leads us to believe it is an ocean world, as well as it being fortunately positioned within the goldilocks zone of its star. Characteristics similar to these make planets outside our solar system potentially habitable, which is why scientists tend to study them extensively. According to NASA's Kepler Space Telescope, "20 to 50 percent of the stars in the sky are likely to have small, potentially rocky planets in their habitable zones." Using Kepler Space Telescope data, we can estimate that 300 million planets have the potential to be habitable, the closest of which could be 20 light years from Earth.

The second category of exoplanets consists of super-Earths, which are rocky planets more massive than Earth yet lighter than ice giants such as Neptune and Uranus. Super-Earths can be up to 10 times the mass of Earth as well as twice the size. A Super-Earth's category is based primarily on its size in comparison to terrestrial planets, which are categorized due to their composition. There can be many different types of super-Earths, from rocky planets to gaseous neptunes to ocean worlds—the compositions can range drastically.

The third broad classification of exoplanets is Neptunian planets, which (similar to super-Earths) are categorized based on size rather than composition. Neptunians, as their name suggests, are a similar size to Neptune or Uranus, yet smaller than gas giants like Saturn and Jupiter. While these planets have a broad range of characteristics, their atmospheres tend to be mainly composed of helium and hydrogen. However, their cores tend to be rocky with a composition of metals. The reason why Neptunians have a variety of different sub-classifications is because they are categorized mainly on size and their atmosphere, which creates sub categories such as mini-Neptunes, warm-Neptunes, and hot-Neptunes. Because planets like Uranus and Neptune contain the chemical compounds methane, ammonia, and water in a frozen form, they are often referred to as "ice giants." Neptunian planets are more likely to form in the outer areas of planetary systems, where the isolation of the planet creates the icy exterior. While Neptunians are the least likely to be habitable, they provide information on the earlier ages of the Universe, such as how certain planetary systems formed and the gravitational shifting within orbits.

Lastly, there are gas giants, which are planets roughly the size of our Saturn and Jupiter. However, they can be much larger. Gas Giants' atmospheres are composed mainly of hydrogen and helium, making them much larger in size than Earth. Their sub-categories include hot-Jupiters, warm-Jupiters, and super-Jupiters, which are all specified categories based on temperature or size. Instead of having a solid surface, they have a solid core and a surface made of a mixture of gases. Gas giants can range from very long orbital periods to extremely short orbital periods of just 18 hours to complete the trajectory around their host star. Unlike our own solar system, where Jupiter and Saturn are located just outside the asteroid belt, roughly 1.2 AU to 2.2 AU from the sun, gas giants have been discovered at very close and very far distances orbiting their host stars. It is celestial oddities such as these that make humans question the formation of the solar system. Do planets form farther from the star and migrate inwards? Or are they forming a short distance from the star and migrating further away? We are able to explore the possibilities of planet migration through gas giants because there is no necessary distance for the planet to be located.

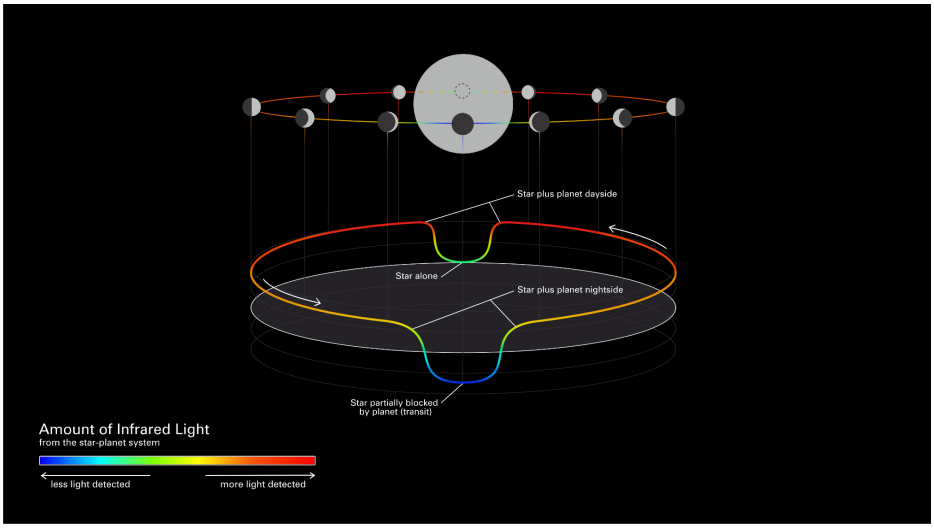
These ideas lead us to the question: How can we detect these planets? There are five main methods of detection: astrometry, radial velocity, transit photometry, gravitational microlensing, and direct imaging. Astrometry tracks the star's position and studies the "wobble" of the host star based on exoplanet pull. The wobble is then compared to the stars in the background, which allows us to estimate a planet's mass as well as its orbital inclination. However, astrometry requires highly precise data, making it more susceptible to error. For that reason, only a small number of planets have been discovered through it. Radial velocity is very similar to astrometry in that it tracks the star's "wobble" as well; however, it is different in that when viewing exoplanetary systems from the side,

we use radial velocity, whereas astrometry is used when the system is viewed from above. This is because in radial velocity, we are essentially collecting the different wavelengths of the planet: the red and blue shift. When the planet moves towards us, we view the wavelength in blue shift, versus further away, which creates a red shift. By measuring the change in wavelength, we are able to calculate the velocity of the planet, and we can then collect information on the planet's mass and its orbit. Transit photometry is used when a planet passes in front of its host star. When this occurs, there will be a slight change in the luminosity of the star or a "dip". This allows us to detect the planet. However, the only flaw to this method is that it takes the planet's orbital period (however long that may be) to track it again. Gravitational micro-lensing involves the capturing of the bending of light of a different star as it passes behind a host star. When two stars align, the star behind the host star's light curves around it due to Einstein's theory of general relativity. If a planet is in the vicinity of the host star, the light will bend around the planet as well, allowing for its detection. While many planets have been discovered through gravitational microlensing, it is unrepeatable because the two stars will never align again, making it a one-time opportunity to discover it.. Finally, we have direct imaging, which involves using the light of the planet itself to identify it. Because the planet emits its own infrared signal, it can be captured by telescopes and separated from the star signal. However, direct imaging can be incredibly difficult to do because the light from the host star can oftentimes interfere with the detection.

When the idea of potential planetary systems outside of our own comes to mind, the question of habitability often arises. In order for a planet to have the potential for habitability, it must have a few specific characteristics, including living in the "goldilocks zone" or the orbital radius interval at which liquid water can exist. Not too close, yet not too far from the host star. Where the goldilocks zone is located is also dependent on the size and luminosity of the host star. The second characteristic would be the composition of a planet, which is very important in contributing to the sustainability of life. Using transmission spectroscopy on planets, we are able to determine the composition of the planets based on the elements they contain. The most important are biological elements such as nitrogen, carbon, and oxygen. We would also have to ensure the atmosphere is sustainable: that it has a sufficient balance of greenhouse gases to keep the climate controlled and that it has enough pressure to preserve the liquid water.

There are currently many new discoveries involving exoplanets; a few of the space missions have made incredible contributions. The Kepler Space Telescope, launched in 2009, was one of them (its first planet searching mission.) It surveyed planets and solar systems, as well as cataloging possible habitable zones. The mission went on for 9 years until October 30th, 2018, when it emptied its supply of hydrazine fuel in totality. The TESS, or the Transiting Exoplanet Surveying Satellite, was a mission run by MIT which launched in 2018. It searched for visible light wavelengths and completed that task so well its mission was extended through 2028. Lastly, the Nancy Grace Roman Space Telescope, which launched on August 30th, 2026, will investigate exoplanets and dark matter. It will use the methods of gravitational microlensing, direct imaging, and transit method in order to block starlight and locate exoplanets directly. Its field of view is 100x larger than that of the Hubble Space Telescope, allowing for more data capture.

Exoplanets are an important part of modern astronomy and allow us to have a better understanding of our Universe and planetary systems. By identifying different types of exoplanets, we are able to broaden understanding of the possibilities of extraterrestrial life. It's possible to have a planet orbiting two host stars, it's possible to have a planet orbit its star in less than 18 hours, and it's possible to have a planet with a density of 0.093g/cm^2. As space technology advances, so does our grasp on the limitations of, and potentials for, life on other planets. The universe is filled with trillions of worlds we've yet to discover, and we've only just begun to look.



NASA, ESA, CSA, DANI PLAYER (STSCI) [8]

The Types of Prion Diseases

AKARI HIGASHIDA '28

What are Prion Diseases?

Prion diseases (PrDs) are triggered by misfolded proteins called prions. PrDs are neurodegenerative diseases with symptoms including brain disorder and dementia, which often ultimately lead to death. Newly formed prions are uniquely troublesome because they can misfold nearby healthy proteins. These diseases are extremely hard to identify and cure because the prions often damage the brain's core functions before symptoms can even begin to show. Although prions are simple proteins with no genetic material like DNA or RNA, they are highly resistant to extreme conditions. One paper describes prions as "remaining active at temperatures exceeding 600°C and resisting conventional sterilization methods such as autoclaving" [1]. Autoclaving uses heat and steam to destroy microorganisms such as bacteria, viruses, and fungi, but it cannot completely remove prions.

PrDs, which affect both animals and humans, fall into three major categories of causation: sporadic, genetic, and acquired. The most common form of PrD is sporadic, where prions appear randomly. Genetic PrDs occur when a mutated form of the PRNP gene, which encodes prion proteins, gets passed down. Acquired PrDs, on the other hand, come from external sources as they are transmitted by contaminated food or medical equipment; transmission is uncommon but it is still a major cause of serious outbreaks. Although there are no fundamental cures to these diseases, scholars are researching ways to prolong the lives of patients by slowing down the progression of symptoms.

Creutzfeldt-Jakob Disease

First discovered in the 1920s, Creutzfeldt-Jakob disease (CJD) is a type of PrD that is only found in humans. Its symptoms vary from behavioral changes to mental and motor impairment. CJD is a fatal disease that progresses quickly. In fact, roughly 70% of people with CJD die within one year of getting the disease [3].

Although most cases of CJD are sporadic, CJD outbreaks are also often caused by the reuse of contaminated surgical equipment and transplantation of tissue containing prions, a testament to the poor medical practices of some clinics. However, because of CJD's long latency period, which is estimated to be 10 years [4], the detection of the source of transmission is delayed. New medical practices such as replacing the transplantation of pituitary glands with DNA-derived hormones avoid prion contamination, reducing acquired CJD prevalence.

Bovine Spongiform Encephalopathy (BSE), also referred to as "mad cow disease," is a variant of CJD that led to a major outbreak in the U.K. in the 1980s and 1990s. Scientists believe that the cause of this disease was cattle being fed prion-infected meat. The impact of this epidemic was devastating as "more than 184,000 cows in the U.K. died from BSE between 1986 and 2015" [5]. To combat these outbreaks among animals, regulators imposed widespread bans on recycling spinal columns and infected livestock tissue into animal feed, an action that drastically reduced the number of BSE cases reported.

Fatal Familial Insomnia

Fatal Familial Insomnia (FFI) is a rare genetic PrD that damages the thalamus, a part of the brain that regulates sleep. Its symptoms include sleep difficulties, memory loss, and muscle twitching. FFI is a life-threatening hereditary disease that leads to progressive brain degeneration. The prions drive the nervous system into a state of overactivity, inducing anxiety, high blood pressure, and increased heart rate. In addition, since sleep plays a vital role in the human body, the lack of sleep caused by FFI negatively affects one's overall well-being as the brain is unable to recharge the energy required for proper bodily function.

The Kuru Epidemic

Cannibalism is known to be the origin of the Kuru epidemic, which "wiped out about 30% (at least 3000 individuals) of the Fore people of Papua New Guinea in the 20th century" [1]. This epidemic started among the Fore people, an ethnic group of New Guinea, who practiced cannibalism as part of their funerary rituals. The consumption of the brains of their ancestors was a holy act of commemorating their lives and passing down their wisdom to younger generations. However, this tradition triggered the transmission of prions to the bodies of the Fore people, spreading the disease. Although the ritual was discontinued by the Australian government during the 1950s and 1960s, new cases continued to be reported because of kuru's long latency period, which ranged from approximately five to forty years.

The Search for a CJD Cure

Researchers Sonia Vallabh and Eric Minikel found out that the introduction of small interfering RNA (siRNA) can be effective as a cure for prion diseases. The siRNA cure functions by cutting the messenger RNA that contains the genetic instructions for making prion proteins, preventing or delaying the misfolding of proteins. Minikel explains that they "want to go upstream and target the RNA molecule that makes the protein" because the cells that create prions are hard to detect [7]. This treatment is entering clinical trials, and Vallabh and Minikel hope that their research data will contribute to new discoveries in the whole field.

Although prion diseases are rare, their highly resistant nature has troubled the pursuit for an effective treatment. Researchers continue to seek approaches that could provide a cure for these diseases for patients in the near future.

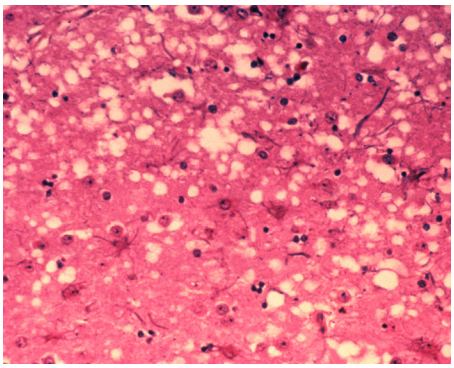


Figure 1. BSE-affected brain tissue shows microscopic holes that give it a spongy appearance.

DR. AL JENNY, USDA APHIS, VIA CDC; PUBLIC DOMAIN [8]

An Overview of CRISPR

RUSSELL FAN '28

Over the past two decades of scientific research, one significant development in biotechnology has been the transformation of CRISPR (Clustered Regularly Interspaced Short Palindromic Repeats) into a gene-editing technology. Although commonly associated with genetic modification, CRISPR is, at its core, a delicate system used by bacteria and archaea to protect themselves from invading phages and plasmid. First discovered in the late twentieth century, this process begins when a bacterium encounters a plasmid and stores its information in the DNA-derived spacers. When the bacterium recognizes the invader, it expresses a unique RNA and interferes with the invading genomes. For many years, scientists did not fully understand how the RNA molecules were produced and guided to the invading plasmids. Through extensive studies on this immunity system in the 2010s, however, scientists were able to answer these questions and find ways to mimic and use it to edit genes.

In 2011, Deltcheva et al., while studying the CRISPR system of Streptococcus pyogenes, took one of the first steps towards developing the gene-editing technology we know today. While investigating how pre-crRNAs (precursor CRISPR RNA) are cut into smaller functional pieces, the scientists identified a trans-encoded RNA named tracrRNA(trans-activating CRISPR RNA). This RNA has a sequence that is complementary to the repeat sequence in the pre-crRNA, which would pair up together to create a double-stranded RNA. In a mutant strain with the absence of tracrRNA, crRNA is no longer produced, suggesting that tracrRNA is important within this process.

In addition to tracrRNA, RNase III, an enzyme involved with processing RNA in bacteria, and Csn1, a CRISPR-associated protein, are also crucial to the maturation of crRNA. RNase III is essential for the cutting of paired RNAs, while Csn1 assists with the pairing of tracrRNA with pre-crRNA. Bacteria lacking any of these components were found to be unable to protect themselves from invading plasmids. Together, tracrRNA, RNase III, and Csn1 were shown to be necessary to produce mature crRNA. Producing the crRNA, however, is only the first step. The next question is how this RNA uses information stored in its sequence to direct the CRISPR-associated proteins (Cas) towards invading plasmids.

A 2012 study by Jinek et al. reveals how tracrRNA and crRNA play important roles in the process of targeting the invading gene. This study was one of the first to demonstrate the foundations of modern genomic technology. Cas9, a CRISPR-associated protein that has the function of cutting targeted DNA, needs both crRNA and tracrRNA to cut the target DNA of the invading plasmid. TracrRNA assists with forming the RNA that interacts with Cas9, crRNA contains information that determines which DNA Cas9 should target, and Cas9 is the protein that binds to the RNA and cuts the invading plasmid. When the Cas9 protein arrives at the site, it utilizes its two nuclease domains, HNH and RuvC, to create double-stranded breaks. The HNH cuts the strand that is complementary to the crRNA-guide sequence, while RuvC cuts the noncomplementary strand.

Though Cas9 relies on two separate RNAs in nature, the researchers investigated the likelihood of connecting the two required RNAs into a single RNA molecule that could be modified to target a specific gene. Connecting the 3' end of crRNA to the 5' end of tracrRNA mimics the dual-RNA structure that guides Cas9, known as chimeric RNA which has the ability to direct Cas9 to targeted DNA sequences. From their research, Jinek et al successfully created five different chimeric RNAs that are designed to target different DNA sites. Thus, Cas9 acts as the scissor cutting the targeted DNA sequence, while the single chimeric RNA holds the information of which DNA is to be targeted. It allows scientists to change the chimeric RNA to target different DNA, which is the fundamental idea of CRISPR as a gene-editing technology that most people recognize now.

Nowadays, CRISPR technology is a standard method for biological research. For instance, in the field of microbiology, scientists often create knockout mutants of a specific gene in bacteria to investigate the significance of the protein that it encodes for. The same programmability is now being applied to humans, which raises various ethical concerns regarding this powerful yet potentially dangerous technology. What began as a defense system against invading plasmids has become a tool to rewrite genetic information, but scientists must decide where to draw the line.

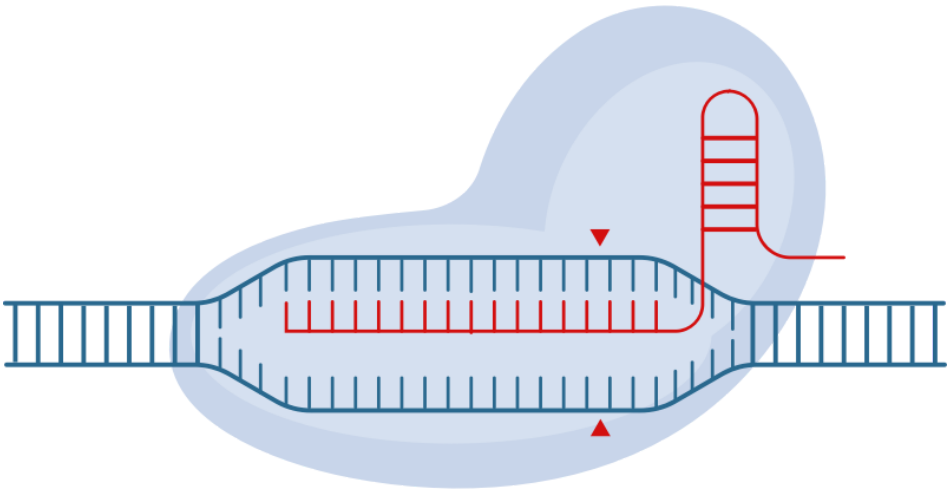


Figure 1. Cas9 uses guide RNA to target a DNA sequence and cut both strands.

MARCEL TISCH, VIA BIOICONS; CC0 [3]

Origin of Life: Spontaneous Proliferation?

KRYSTAL ZHANG '29

How did life originate on Earth? Did life really start from nothing? Was it just luck and magic that created human beings and all the other creatures? These questions provoked a heated debate about the origin of life on Earth. Some believe life appeared as a result of the combination of chemicals on primitive Earth. Others propose that substances from outer space potentially paved the path for life. Still, others think it's just a mix of serendipities and time. Scientists are not close to knowing the exact answer and they may never find the key to this mysterious door. Yet, knowing more about the origin of life on Earth and better understanding where humans came from acts as a vital part to the whole human race. It is somewhat unmeaningful and hollow to live a life not even knowing the most significant part of ourselves – life or human origin. Led by the question "How did life first start on Earth?", this article will expand on research done and explore the unknown past. Abiogenesis and biogenesis are both possible based on various pieces of evidence. In the following, an elaboration on several prevalent theories and experiments will be provided as possible explanations of this mystery.

DISPROVAL OF SPONTANEOUS GENERATION

While it appeared that abiogenesis could explain the creation of life on Earth, many theories and experiments refuted spontaneous generation. Spontaneous generation was disproved through the execution of various experiments and verification of significant theories. After cultivating and enhancing the precision of experiments, results consistently showed that life or organisms can't arise spontaneously.

According to Explore Yeast [6], the development of the Germ Theory of Fermentation and Pasteurization aided Louis Pasteur to disprove abiogenesis. The Germ Theory of Fermentation stated that anaerobic organisms or organisms surviving without oxygen caused fermentation. For instance, yeast was able to live in the absence of air and produce alcohol from sugar. In addition, fermentation occurs only when there are living microorganisms, growing due to the spores in air or on food. This discovery also helped develop the renowned process of "pasteurization". Pasteur implied that if heating killed most of the bacteria, then it's unlikely for a liquid to be spoiled. In other words, fermentation is not caused due to spontaneously generated bacteria, but due to the surviving organisms that produced acid [6].

Furthermore, Pasteur conducted an experiment that further debunked spontaneous generation. He used a swan-necked flask that allowed air to go into the heated broth while keeping bacterial spores out. The result showed no chemical changes or growth of anything in the broth. On the other hand, when Pasteur tilted the flask on its side and allowed access of dust into the heated broth, bacteria growth contaminated the broth. The same would happen if the neck of the flask was broken exposing the liquid to non-filtered air. Overall, this showed that bacteria appearance did not arise from spontaneous proliferation [7].

To better illustrate the point, two other experiments consolidated this refutation against spontaneous generation. Firstly, Francesco Redi proposed that maggots didn't spontaneously generate from rotting meat and supported his opinion with an experiment. Initially, he placed meat in many jars. There were three types of jars, some were left uncovered, some were covered with gauze, and others were sealed with a lid. Gradually, maggots were present in the first two groups of jars but not in the ones that were sealed. He concluded that maggots do not spontaneously arise from meat, because only the ones that flies have access to appeared to have maggots [7]. Plus, Lazzaro Spallanzani demonstrated that microbes do not spontaneously generate. Since he believed that microbes could move airborne, he contended that the microbes that appeared in an experiment conducted by John Needham (an English biologist in favor of spontaneous proliferation) is due to the broth's exposure to air after boiling but before the flask had been sealed. Spallanzani then devised an experiment, where he placed the broth in a sealed flask. After that, he eliminated air from the flask and boiled or sterilized the heated broth. As a result, no microbes appeared in the broth. Undoubtedly, this was a huge blow for spontaneous generation [7].

Based on the many theories and experiments elaborated above, spontaneous generation seems to be an unfeasible explanation for the origination of life on primitive Earth.

This disapproval theory against spontaneous proliferation is indeed persuasive, but arguments in favor of spontaneous proliferation are also present, such as the instances provided below.

PRIMORDIAL SOUP

In 1940 Russian scientist Alexander Oparin and English geneticist John Haldane hypothesized another theory of how life originates – the theory of the primordial soup. Literally, it means a bowl of soup from ancient times. Alexander Oparin and John Haldane theorized that life started in the primordial ocean. The mix of gases in the atmosphere and the energy from lightning strikes allowed the primitive water to be rich and organic, creating amino acids found in protein (an element that all living things have). Over periods of hundreds of years, life became possible to be created spontaneously in the ocean. Amino acids contain nitrogen and hydrogen, and those 2 elements did appear in the primordial time [3]. Hence this theory is reasonable.

In 1952 Stanley Miller, a graduate student from University of Chicago, with Harold Urey, a Nobel laureate in chemistry, conducted a famous experiment that proved life spawned from the primordial soup. Miller and Urey put ammonia (NH_3), methane (CH_4), and water vapor in an enclosed container to simulate the environment in primordial time. Then they put electrical sparks through the container to emulate lightning. Amino acids, which are substances that are found in protein, were soon observed to have formed [3]. These experiments demonstrated the

process of how life potentially formed in support of the primordial soup theory.

HYDROTHERMAL VENTS

Similar to the hypothesis of abiogenesis and spontaneous proliferation is a second postulation of hydrothermal vents. Hydrothermal vents allowed life living in the deep ocean and in extreme environments to produce energy without the energy from sunlight. In other words, with the help of submarine vents, living organisms can be formed deep in an oceanic world with no sunlight and the help of above-sea-level heat.

According to an article published by Heather Scoville [4], these types of organisms are extremophiles that can live in the severest of conditions. Hydrothermal vents are structures in the bottom of the ocean, existing in extreme conditions. The vents were capable of making their surroundings extremely hot, hence the word "thermal" in its name. Life forms that live in and near these vents need and have adaptations that enable them to thrive in these harsh conditions of heat and pressure.

Since sunlight cannot reach to the depths of these structures, there had to be another energy source for early life that may have formed there. A potential energy source lurks behind the vents' chemical compositions. Hydrothermal vents contain chemicals that aid in the occurrence of chemosynthesis—a way for organisms to create their own energy similar to photosynthesis that uses chemicals instead of sunlight to make energy [1].

Synthesizing the amount of heat and pressure in these areas, along with the types of chemicals available, life can be created and changed relatively quickly. Scientists further validated this hypothesis by successfully tracing the DNA of all currently living organisms back to a common ancestor of extremophiles that inhabited the hydrothermal vents [4].

SEEDED BY METEORITES

A final and third hypothesis of the origin of life is a mix of luck, time, and meteorites. It is helpful to start thinking about these questions: Why do meteorites have the ability to carry life? Why can life be carried by meteorites?

The first meteorite drifted through the universe in the form of a comet. The surface of the comet was covered in ice, which froze and in turn protected the preservation of the carried life. This is also one of the reasons why life did not melt when a comet entered the atmosphere, where intense heat is produced from friction due to movement. When the ice layer on the surface of the comet melted, the remaining un-melted meteorite blocks brought the life forms to Earth from outer space.

Some people may say that life would melt when passing through the atmosphere, but in fact, microscopic lifeforms like bacteria or viruses have the ability to pass through the atmosphere. For instance, a virus has a protective layer on its surface that is hard enough to protect it from destruction or deterioration when passing through the atmosphere.

Yet, even if bacteria and micro-viruses were introduced to earth, how did they evolve into larger life forms without perishing? How did a tiny bacterium affect the global production of life? Life comes from reproduction and transmission. Research has shown that the bacteria stayed and survived for a period of time after arriving on Earth, during which they diffused to their most primitive form. Infection through this conduit gradually increased the number of bacteria that bred microorganisms, which mutated and grew into other organisms [5].

AN ONGOING PROCESS OF REVEALING MYSTERIES

In conclusion, life origination is still an unsolved puzzle, where efforts in approaching a possible answer are still being made. Scientists and thinkers proposed different theories and provided their own understandings on this subject. Alexander Oparin and John Haldane theorized that life was first created in the primordial ocean by the combination of energy and gases, which was also later verified by the experiments performed by Miller and Urey. Others contended that organisms are carried to Earth by meteorites or basically arose from hydrothermal vents, where creatures thrived under extreme environments. Against these theories and in contradiction to biogenesis, Louis Pasteur conducted experiments and theories, attesting that organisms cannot arise from spontaneous proliferation. He is renowned for his studies on fermentation and extrapolating conclusions from experiments of previous scientists. The theories explained are just a tiny portion of the iceberg. These scientific investigations prove to be a crucial first step towards an understanding of the origin of life and where the human race came from. The subsequent steps about to be taken require the wider society to remember that "The important thing is not to stop questioning," as Albert Einstein put it [9, p. 64].



ALBERT EDELFELT (1885)/WIKIMEDIA COMMONS [8]

HistGramBench: Can AI Pass Mr. Dollhopf's Geometry Class?

HARRY TRAN '28

You need to be able to sketch a triangle to pass Geometry Accelerated at Deerfield. Consider a hypothetical world where AI policies are non-existent. Should students trust an AI agent to read a geometry sketch and complete their geometry homework? Consider this problem from The Teaching of Geometry (1911): reproduce the semicircle and triangle shown in Figure 3a. Before an agent can solve a geometry problem, it needs to "see" the figure correctly and reconstruct it. One way to rebuild these figures is to redraw them as code. TikZ is a drawing language used with LaTeX, the standard typesetting in mathematics. A TikZ drawing is a short program that compiles the details of a figure so that a computer can read it. Today's frontier AI models that read images, known as vision-language models, can write such programs from a picture [1].

The problem is: how can the accuracy of a redrawn figure be objectively measured? The standard method compares pixels, but differences in line thickness can produce misleading results. Code-by-code comparison is impossible because historical diagrams do not have original code.

We introduce HistGramBench, a benchmark for evaluating how accurately AI models reconstruct historical geometry diagrams. It uses an alternative judging method that checks the facts a reader relies on: which points exist, which points lie on which shape, which lines are parallel to each other, etc. The benchmark seeks to answer a question: How much of a figure's structure do AI models get right, and how often do they fail to produce a drawing at all?

Existing benchmarks that turn pictures into code use modern material that has original TikZ code: scientific figures in TikZ [1], charts in Python [8], and web pages in HTML [7]. These benchmarks grade an AI's output on how similar the output looks compared to the answer key. HistGramBench's foundation is built on Inter-GPS, which describes geometry diagrams as lists of objects and relationships [6].

The figures come from public-domain historical articles (Figure 1). Each sample is a single figure cropped from its page. An automated check procedure and screening model are introduced to remove non-geometry crops and duplicates. Our final test set contains 2,507 crops from an original dataset of 411 books (Figure 2).

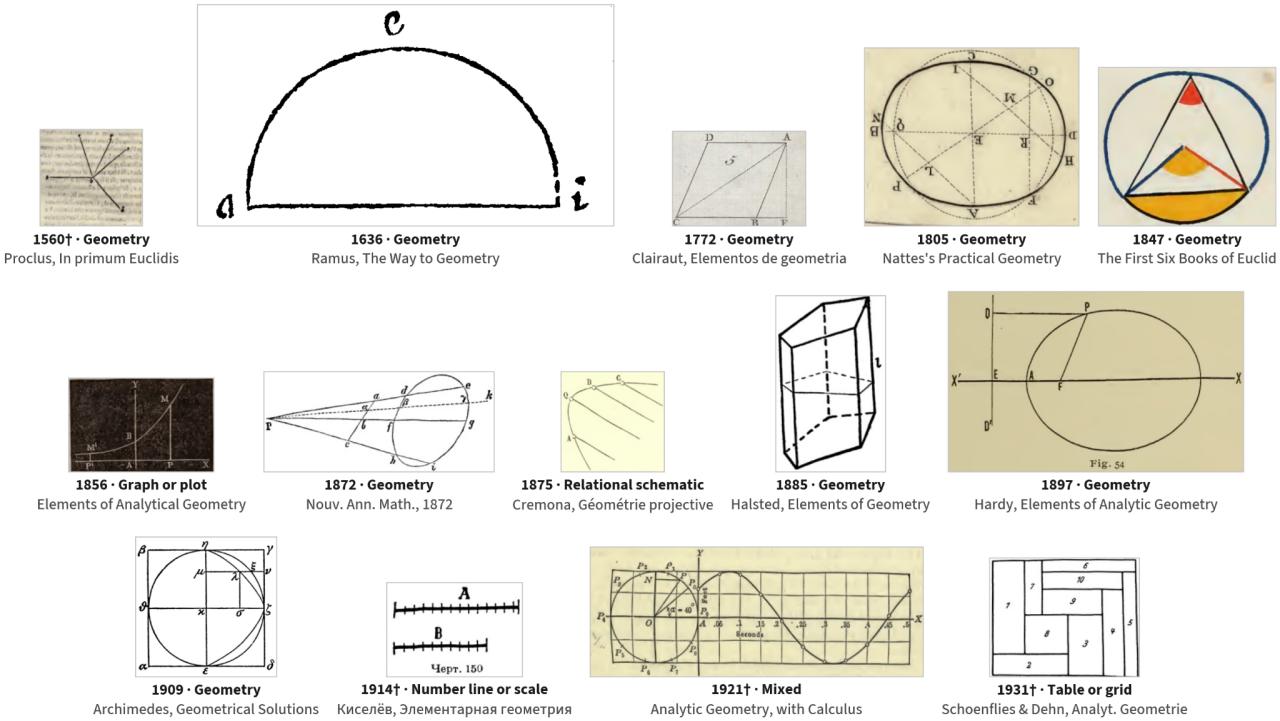


Figure 1. Sample of corpus figures, 1560–1931, with year, figure type and source. †: not in the scored test set.

HARRY TRAN [10]

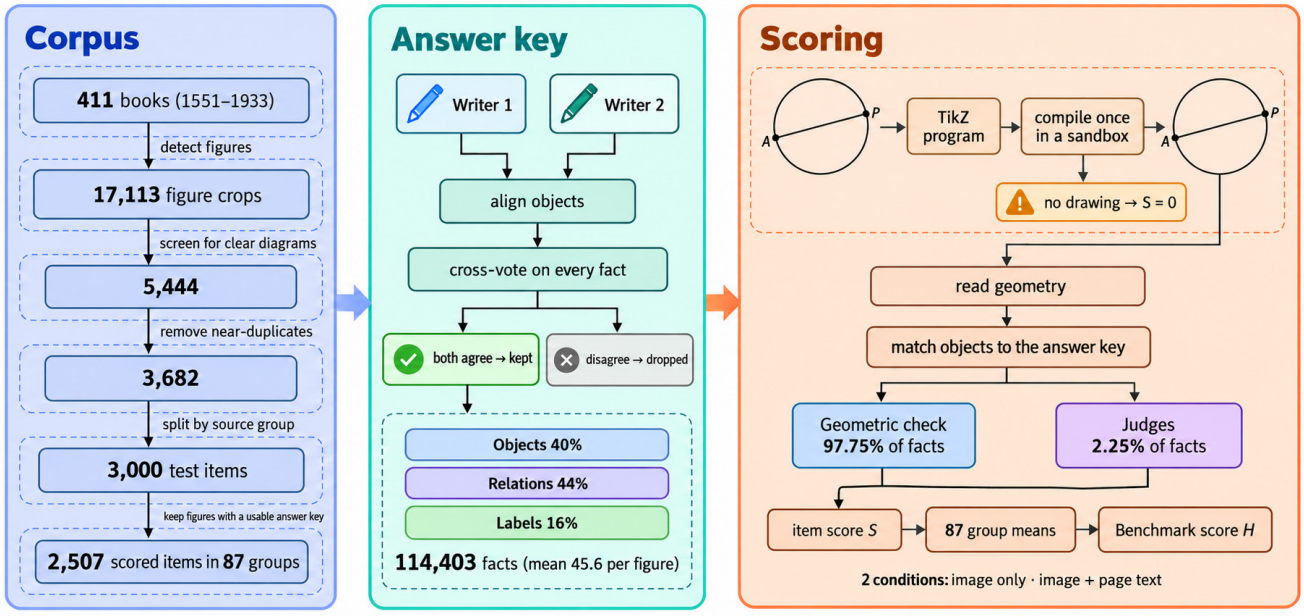


Figure 2. HistGramBench pipeline. Left: corpus building. Centre: answer-key construction. Right: scoring one compiled answer.

HARRY TRAN [10]

Each figure is given to each model in two ways (Table 1). In Track A, the model sees only the figure and is asked to redraw "the mathematical figure the original intended," leaving out stains and printing flaws. In Track B, models receive additional captions and nearby text from the same page. In both tracks, the answer must be a single TikZ drawing. Comparison between Track A and Track B shows us to what degree context influences a model's performance.

Each figure has an answer key: a list of facts of three kinds (Table 2). Entity facts say that an object exists ("there is a point"), relation facts say how objects connect ("Point A lies on the circle"), and label facts show how things are marked ("This point is printed as A"). The answer key avoids recording exact position or size.

Table 1: Task conditions. Page text is present for 1,538 of 2,507 items.

	Track A	Track B
Input	Figure crop	Figure crop, page text
Output	TikZ program	TikZ program
Invariant to	Translation, scale, line width, font, colour	Translation, scale, line width, font, colour

Table 2: Answer-key fact classes (n = 114,403). D: drawing diagonal. 2.25% of facts are decided by the judge panel.

Class	Example	Criterion	Share (%)
Entity	point(P), circle(C)	Present in drawing	40
Relation	on(P, C), parallel(ℓ_1, ℓ_2)	$d \leq 0.01\,D$; $\angle \leq 1.5°$	44
Label	label(P, "A")	Exact string, bound to entity	16

Two self-contained AI models, GPT-6.1 Sol and Kimi K2.5, independently write down facts. Their lists are then lined up, and every fact in the combined list U is voted on. Writing a fact counts as a vote for it unless the writer later rejects it. With vw(f) standing for writer w's vote on fact f, the key is:

$$K = \{\, f \in U : v_1(f) = v_2(f) = \text{support},\ f \text{ consistent},\ f \text{ unambiguous} \,\}.$$

So facts enter the key only when both writers agree. The rule also prefers a shorter, reliable key to an overly complete one. Figures with keys that are too thin or too uncertain are omitted from the test set.

The benchmark takes the TikZ code from the model's answer and runs it on one attempt in a contained environment (Docker) and reads the output picture as a set of points, lines, curves and text (Figure 2, right). If the code fails to compile or contains forbidden commands, the output is considered a complete failure.

The objects in the key are first paired with objects in the drawing. Each fact is then checked by measuring the drawing. For instance, let d(p, x) be the distance from a point p to an object x, and let $\angle(\ell_1, \ell_2)$ be the angle between two lines.

A point counts as lying on a circle when it sits within one percent of the drawing's size from it. Two lines count as parallel when their directions differ by at most 1.5 degrees. The drawing's size is independent of these criteria because distances are compared with the size of the whole drawing. The checking process is only dependent on written facts, so line thickness, font and colour do not make significant differences. Other relations such as right angles are checked with the same methodology. More complex facts such as shaded regions or marks showing equal lengths go to a third independent judge for further corroboration.

A model's performance is measured mathematically. Let K_i be the answer key, P_i the facts reproduced, and X_i the facts excluded because a required object is missing. The set difference $K_i \setminus X_i$ contains the checkable facts. Let g_i equal 1 for a valid drawing and 0 for a compilation failure:

$$S_i = g_i \cdot \frac{|P_i|}{|K_i \setminus X_i|}.$$

The corpus also contains books from adjacent authors so some figures tend to resemble each other. The benchmark tackles this by averaging scores within each group of related books and then averaging the groups:

$$H = \frac{1}{G} \sum_{k=1}^{G} \bar{S}_k,$$

where $\bar{S}_k$ is the average score in group k and G = 87 is the number of groups. The 95 percent range around each result uses the 87 group averages as the sample [3].

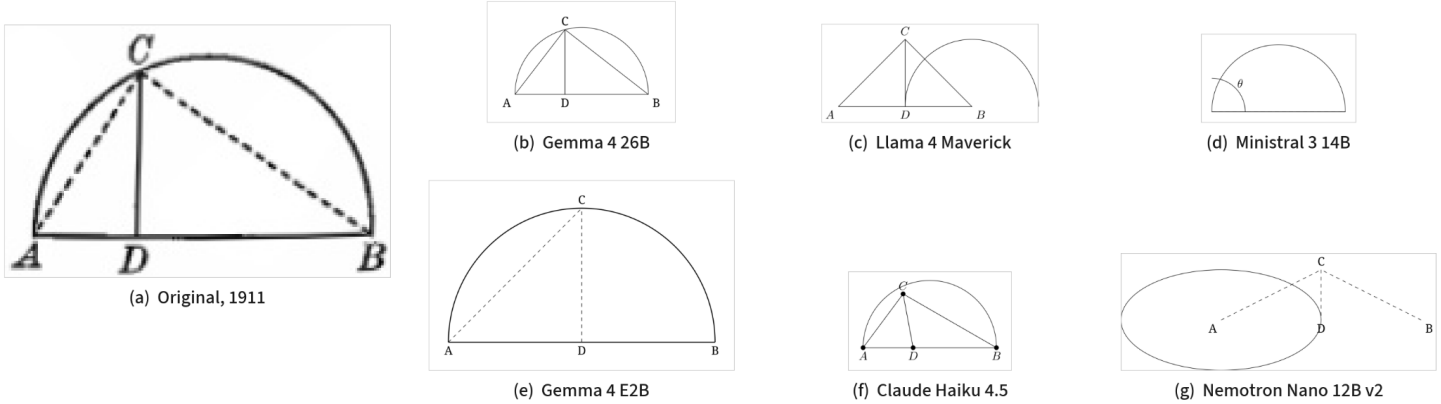
Six vision-language models were tested: Gemma 4 26B, Llama 4 Maverick, Ministral 3 14B, Gemma 4 E2B, Claude Haiku 4.5 and Nemotron Nano 12B v2. These models' outputs shared the same configurations and the same limit on answer length.

Gemma 4 26B does best, with a Track A score of 0.59 (Table 3). Performance of Gemma 4 E2B and Claude Haiku 4.5 is in the same bound through sorting the six into five distinct levels [2].

Many answers failed to compile: Of 2,507 Track A answers, Nemotron Nano 12B v2 ran out of answer length on 651, Llama 4 Maverick introduced forbidden commands on 292, and Claude Haiku 4.5 wrote code that failed with syntax errors on 1,218; in 1,007 cases it left out the line opening a LaTeX document. Models struggled the most with relations.

Adding page text does not have a significant influence on the overall performance of models. Individual models move both ways, with gains from Ministral 3 14B to a loss of 0.08 for Gemma 4 26B (Figure 5), and the five levels of Track A merge into two (Figure 4).

$$\mathrm{on}(p, x) \iff d(p, x) \le \varepsilon D, \qquad \mathrm{parallel}(\ell_1, \ell_2) \iff \angle(\ell_1, \ell_2) \le 1.5^\circ, \qquad \varepsilon = 0.01.$$



(a) Original, 1911 (b) Gemma 4 26B (c) Llama 4 Maverick (d) Ministral 3 14B

(e) Gemma 4 E2B (f) Claude Haiku 4.5 (g) Nemotron Nano 12B v2

Figure 3. Worked example (Track A; The Teaching of Geometry, 1911; 40 facts). (a) Original crop. (b)–(g) Compiled drawings with S = found/checkable facts.

HARRY TRAN [10]

Table 3. Main results (N = 2,507 items; G = 87 source groups). H is the group-mean item score. Valid is the share of outputs yielding a drawing. Recall is shown by fact class. Bold: best; underline: second.

	H		Track A			
Model	Track A	Track B	Valid (%)	Entity	Relation	Label
Gemma 4 26B	**0.589**	**0.511**	**72.7**	**0.592**	**0.538**	**0.648**
Llama 4 Maverick	<u>0.524</u>	<u>0.506</u>	<u>70.4</u>	<u>0.532</u>	<u>0.427</u>	<u>0.582</u>
Ministral 3 14B	0.391	0.495	<u>70.4</u>	0.509	0.395	0.533
Gemma 4 E2B	0.309	0.325	60.2	0.407	0.332	0.450
Claude Haiku 4.5	0.300	0.296	50.8	0.389	0.317	0.384
Nemotron Nano 12B v2	0.197	0.266	51.0	0.325	0.235	0.346
Pooled ΔH (B − A) = +0.015, 95% CI [−0.010, +0.040]						

To see if ranking is dependent on the family of the AI Judges, each judge's model family was removed in turn and the six models were reranked. There was no significant correlation between grading and model family.

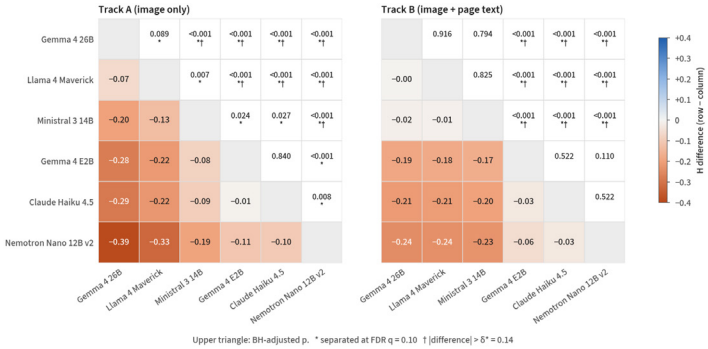


Figure 4. Pairwise differences in H (row − column). Upper triangle: adjusted p. *: separated at FDR q = 0.10. †: |difference| > 0.14.

HARRY TRAN [10]

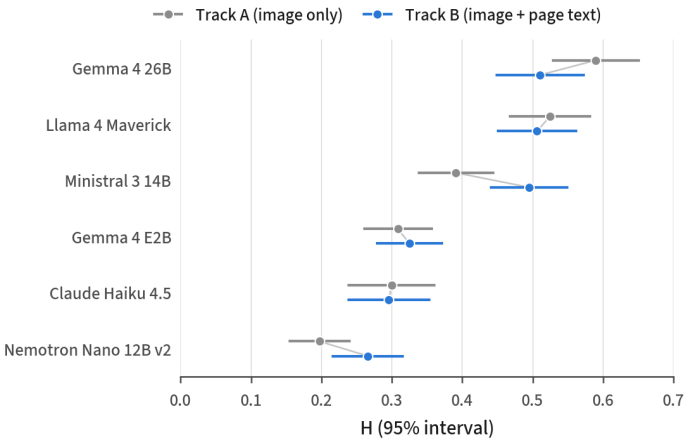


Figure 5. H per model in Track A and Track B, with 95% intervals.

HARRY TRAN [10]

So, can AI pass Mr. Dollhopf's geometry class? Six frontier AI models surely did not, at least not yet. Even the best model gets a large part of each figure wrong, and many answers fail to produce drawings, which is like giving a blank page as a submission. Proprietary frontier models like Claude Haiku 4.5 still fail on fundamentals like leaving out the first line of code, equivalent to not signing the Honor Pledge on the test. If you use AI, whether your school's policy allows it or not, you are setting yourself up to fail geometry class.

For engineers, the quickest step-improvement is configuring the model to produce a valid output. Most failures are mechanical, such as running out of answer length or breaking syntax. In model training, engineers should focus on training models to understand relations instead of just learning how to look at a figure and guess. Fact-level checks in this benchmark can serve as a framework for data that can be used in reinforcement learning. Additionally, researchers should be mindful of page text. It is dependent on individual models, so keeping image-only examples in training can help models learn to read the figure instead of over-relying on context and captions. Finally, bigger does not mean better. Gemma 4 26B, an open-sourced model by Google with only 26 billion parameters, performed better than a proprietary Claude model.

HistGramBench shows that current vision-language models have trouble redrawing historical geometry figures, especially in producing a drawing that adheres to syntax and relations. We hope HistGramBench will encourage work on models that read a figure's geometry with higher precision and grounding from textbooks that are centuries old to a printed homework worksheet due on a Thursday.

Bacteria as Living Circuit Boards

MILLIE HUANG '29

What if bacteria could do math? Would it be able to create algorithms to crash the global economy? Would the human species get taken over by bacteria? Well, bacteria can now do calculations, so who knows what may happen in our future.

On August 17, 2026, researchers at MIT announced their breakthroughs in turning entire bacterial colonies into biological transistors and circuit boards. The team used colonies rather than individual bacteria because individual bacteria lack the metabolic energy to host whole circuits, cell toxicity or growth failure would occur in them [1]. Therefore, the MIT team distributed the workload across multiple specialized bacterial colonies using quorum sensing to connect them.

Background knowledge:

To understand biological computing, it is helpful to understand traditional computing and cellular communication.

Transistor and Logic Gates:

Traditional silicon transistors are electronic switches that use voltage to flip between on and off states. Logic gates are circuits made up of two or more transistors.

Quorum Sensing and Autoinducers:

On the other hand, bacterial transistors rely on quorum sensing, which is essentially how bacteria talk to each other. Bacteria naturally emit small signaling molecules called autoinducers which change the gene expressions of other nearby bacteria, and act as the "voltage" in this specific circuit.

Methodology and setup:

In this experiment, the MIT researchers utilized acyl-homoserine lactones (AHLs), a specific family of natural autoinducer molecules. To achieve a full circuit, the team of scientists engineered five strains of the bacterium *Pantoea agglomerans* (a type of bacteria that resides on plant surfaces [2]). Two strains acted as logical switches (transistors), while three strains served as communication lines (wires).

Placement and spacing:

Using an acoustic liquid handler, the scientists printed five strains onto agar plates in different patterns to achieve different calculations [3].

Layout:

Colonies were set to be about five millimeters apart. The researchers chose the distance because colonies would be close enough that signaling molecules could reach the next colony in the controlled direction while also being far enough away so they wouldn't trigger anything else on the circuit [4].

Passive Diffusion:

When a transistor colony produces the output molecule OHC-14, the molecule exits the cell without using cellular energy. This process of *passive diffusion* is due to the OHC-14 having a nonpolar hydrophobic acyl tail which can easily pass through the lipid membrane of the bacterium allowing for diffusion into the surrounding agar [5].

Components:

Transistor Strains:

As the name suggests, these strains are the transistors of the bacterial circuit. They use three types of AHL molecules: OC-6 as the control input, OC-12 as the data input, and OHC-14 as the output [1].

N-type Transistor Strain:

These strains have their DNA programmed for OC-6 to bind with receptors inside the cell called LuxR-family receptors or other variants like TraR and LasR. They are transcription factors (regulatory proteins) that have binding pockets shaped to fit the 6-carbon tail of OC-6. The activated OC-6 receptors attach to the DNA and trigger the cell to start producing either CinR or RhlR, which are proteins that catch OC-12 with binding pockets designed for grabbing the 12-carbon tails of the molecule. This is the "on" in terms of traditional transistors.

P-type Transistor Strain:

These cells are active by default, meaning they produce the output, OHC-14, whenever OC-12 is present. When OC-6 binds to its LuxR variant repressors, however, the protein physically disables the region in the cell that produces OHC-14, blocking the RNA polymerase from moving forward and stopping the entire biological assembly line that makes OHC-14. This is the "off" in terms of traditional transistors.

OC-12 and OHC-14:

OC-12 is the "target molecule," or the data being processed. Transistors check for its presence to decide whether or not they should generate outputs, OHC-14 in this case. If the transistor is on and it detects the OC-12, the cell activates an enzyme called AHL synthase that synthesizes OHC-14 using materials in the cytoplasm. Then the OHC-14 passively diffuses into the agar and travels until it reaches a neighboring colony.

Relay Strains:

Relay strains connect the transistor cells together like wires on a traditional circuit board. They convert the OHC-14 (which cannot be read as an input by another transistor) into molecules that can be read. Each strain has receptor proteins from the LuxR family that are shaped to catch OHC-14. The DNA gets unlocked as the proteins bind with the molecule and the cell starts to manufacture a synthase enzyme that produces OC-6, OC-12, or OHC-14 depending on the strain. These molecules move out of the cell wall and travel through the gel to hit the next transistor [3].

One type of relay strain translates OHC-14 to OC-6. They allow the calculations from the previous transistor to flip the switch of the second transistor. The second one translates OHC-14 to OC-12. They allow calculations from the first transistor to be the data stream of the next transistor. The third strain makes more and stronger OHC-14 after receiving OHC-14. They are amplifiers used to reduce the effects of the natural fading and diluting of chemicals as they travel through the gel.

Significance and the Future:

By combining these five strains, the MIT team connected up to 24 bacterial colonies to perform operations such as binary addition. The scope of these activities is huge, with senior author of the MIT paper and head of MIT's Department of Biological Engineering Christopher Voigt noting that, from a logical standpoint, "there's nothing that your iphone can do that these circuits couldn't do." [1, "Complex calculations" section, para. 3].

While logically capable, biological computation is limited by speed. A single calculation takes around eight hours because of the time needed for protein synthesis and molecular diffusion. However, there is immense potential for expansion in environmental and medical fields.

You can be rest assured that bacteria aren't taking over the world just yet. But as this technology advances, the boundary between living organisms and computing systems will continue to blur.

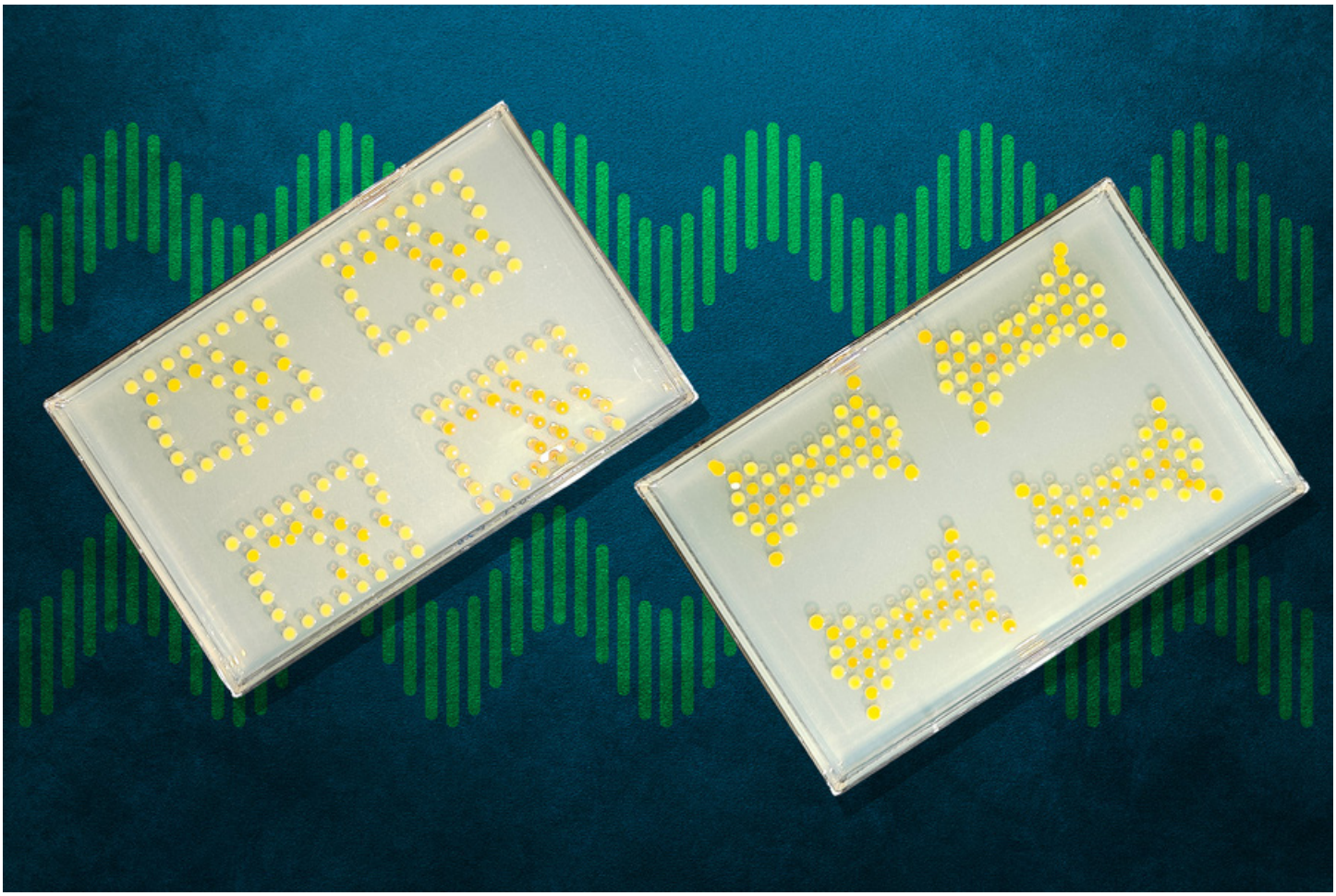


Figure 1. Living circuit boards made from engineered bacterial colonies.

COURTESY OF THE RESEARCHERS, EDITED BY MIT NEWS, CC BY-NC-ND 3.0 [8]

Quantifying Error in Harmonic Reduction Systems

CARTER HE '28

Abstract

Robotic arms require extreme precision to complete important and specific tasks. Yet, harmonic reducers, an extremely accurate type of gearbox that reduces backlash[1], still struggle to achieve the necessary accuracy for complex tasks. Their sources of error fall into two major categories: static error, caused by imperfections in system construction and assembly, and dynamic error, caused by phenomena such as load's[2] twisting effect on the flexspline[3]. Li et al. (2025) designed an experiment to quantify the error stemming from the straining of the flexspline under significant load. Their model predicted the machine error with 93-96% accuracy, and their results demonstrated that load had a greater effect on the accuracy of the harmonic reduction than manufacturing error did; sudden changes in load significantly affected the performance of the arm. Their results suggested a stiffer flexspline be used to reduce backlash and stabilize the load, and dynamic software adaptation to correct quantified load-induced error.

Introduction

Robotic arms require extreme precision to complete important and precise tasks. Small errors in angle compound as the target point moves further away from the axis of rotation. In robotic arms, which often stretch as long as four meters, small errors in angle can be significant. A typical error value in robotic arms using harmonic reductions of one arcminute (1/60th of a degree) can cause errors as large as 0.6 mm at the top of a two meter, a magnitude large enough to miss a target or drop a part during a space repair operation.

Most industrial and space arms use harmonic reductions because of their compact, lightweight design and their highly efficient reduction, enabling large torque ratios in one gear to gear interaction. The secret lies in a flexible rack [^1] which rotates by meshing its teeth with a rigid circular spline with more teeth. The flexible nature of this flexspline, however, is also the source of the harmonic reduction's greatest inaccuracy: rotational inertia[4] and sudden changes in torque warp the shape's structural integrity.

Earlier studies attributed error in harmonic reductions to flaws in manufacturing and construction such as misshapen teeth and poorly coupled components. These errors cannot be addressed once the system is fully constructed. Li et al. (2025), however, hypothesized dynamic error to be more significant than static error, designing an experiment to prove their claim by quantifying both error types.

Fundamentals of harmonic reductions

Harmonic gearboxes are primarily made of three different parts: a wave generator, a flexspline, and a rigid outer/circular spline.

The wave generator is often the input for the system. Due to its oval shape which forces meshing of a number of teeth between the flexspline and the circular spline, the system is able to control precise and targeting movement while producing the large torque gear ratios that harmonic reductions are famous for (Harmonic Drive LLC, 2021).

The most defining characteristic of the harmonic reduction is the flexspline. As suggested in its name, the flexspline boasts impressive flexibility which it uses to hug the elliptical shape of the wave generator while also meshing with the circular spline. In order for it to function as intended, it often has two fewer teeth than the circular spline. The flexspline cannot be fixed upon the wave generator as it would lead to zero reduction in the system.

The circular spline serves as the stationary mechanism that the flexspline uses for movement. When the wave generator's elliptical shape pushes two sections on opposing sides of the flexspline outwards, it pushes the offset teeth into each other, slightly shifting the flexspline to match the circular spline at those points.

The actual reduction produced comes from the offset and difference in teeth between the flexspline and the circular spline. In Li et al. (2025)'s experiment, the scientists used an outer ring with 242 teeth and a flexspline with 240 teeth, creating a shift of two teeth with every full rotation of the wave generator. Therefore, the gear ratio, which will be referred to as n, can be found by dividing the number of teeth of the circular spline by the difference in teeth between itself and the flexspline. This calculation produces a value of 121; the motor must turn 121 times to produce a full rotation in the flexspline.

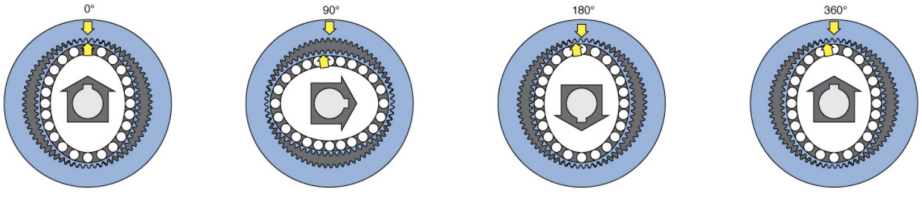


Figure 1.1. Parts and interactions of harmonic reducers. Source: Harmonic Drive LLC (2021) [1].

Terms: [1] Backlash: lost motion due to under-rotation. [2] Load: external torque applied upon the output.
[3] Flexspline: flexible gear that deforms to serve as the output. [4] Rotational inertia: resistance to rotational motion.

Methodology

Using the formula below, Li et al. (2025) focused on transmission error, which describes the position of the arm relative to where it should be under ideal circumstances:

$$\tilde{\theta} = \theta_h + \theta_k = (\theta_m / n) - \theta_l$$

$$\theta_h = \tilde{\theta}_p + \tilde{\theta}_s$$

$\tilde{\theta}$	Transmission error	θ_k	With load step change
θ_m	Input angle	θ_h	Without load step change
θ_l	Output angle	$\tilde{\theta}_p$	Static error
n	Transmission ratio	$\tilde{\theta}_s$	Dynamic error

Li et al. (2025) decided to analyze both static and dynamic error separately so as to isolate and measure the individual effects of each.

To model the error, the scientists ran experiments under a low rotational speed of 5 rpm with a 67 Nm load [^2]. The setup consisted of a fixed wave generator, held in place by code, which fought against any applied load. While the first motor held steady, a second motor gradually twisted output—the flexspline—from 0 Nm to 67 Nmto -67 Nm, and finally back to 0 Nm once more as the sensors tracked torque and rotation, allowing Li et al. (2025) to understand and model flexspline's springiness.

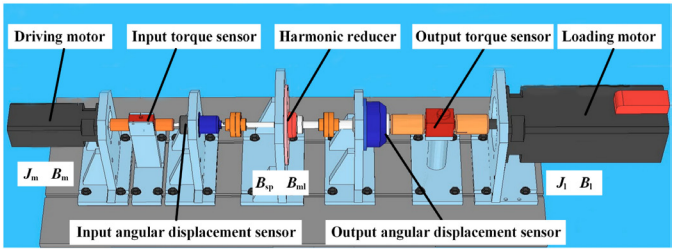


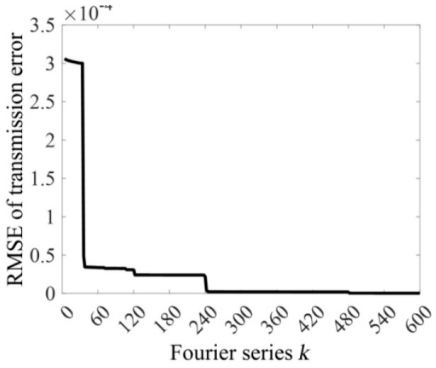
Figure 1.2. Experimental setup. Source: Li et al. (2025), CC BY 4.0 [2].

Static error

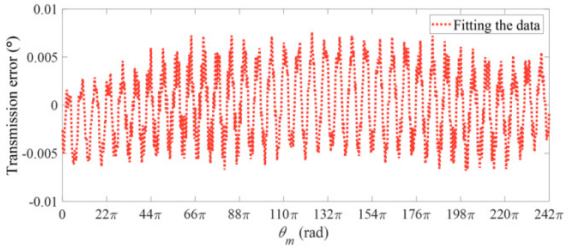
Since static affects the system at the same spot of rotation with each axle turn, Li et al. (2025) were able to use a Fourier series expansion [^3] to model its effects:

$$\tilde{\theta}_p = \frac{a_0}{2} + \sum_{n=1}^{k=240} \left[a_n \cos(n\theta_m) + b_n \sin(n\theta_m) \right]$$

To identify the order of the Fourier expansion, Li et al. used Root Mean Square Error (RMSE) [^4], plotting it against a Fourier expansion with a variable order [^3.5]. Their results showed that RMSE of the driving error dropped only nominally following the 240th order.



The scientists also tested the effects of static error upon a system with zero load. The model identified the lost motion caused from imperfect meshing and backlash caused by manufacturing error to be 1.341 arc min



Static-error plots. Source: Li et al. (2025), CC BY 4.0 [2].

Dynamic Error

To test for the dynamic error, Li et al. (2025) took the data from the setup of the fixed input motor and moving secondary motor, and they analyzed the data as a plot. The returned model showed a slightly non-linear curve, so the scientists fitted it along a fourth degree polynomial to model the non-linear nature of the flexspline's elasticity:

$$T_l = K_4\theta^4 + K_3\theta^3 + K_2\theta^2 + K_1\theta + K_0 \qquad T_l = \text{Torque}$$

Using the identified values of K, they found for Elastic Potential Energy formula of the flexspring using equations:

$$\tau = -\kappa \cdot \theta \text{ and } W = \int_{\theta_1}^{\theta_2} \tau \, d\theta$$

Key:
τ = Torque
κ = Spring Constant

Combining these two formulas, Li et al. arrived to the following:

$$V = \int_{\theta_1 - \frac{\theta_m}{n} + \tilde{\theta}_p}^{0} K\theta \, d\theta$$

They then solved for the kinetic energy of the spinning ends

of the system as well as total energy losses from dampening and friction, defining them respectively in the formulas below:

$$E = \frac{1}{2}J_m\dot{\theta}_m^2 + \frac{1}{2}J_l\dot{\theta}_l^2$$
$$D = P_B + P_f$$

J = Moment of inertia

P_Q = Elastic structural

P_e = Gear meshing frictional loss

P_h = Harmonic Bearing frictional loss

For dampening error and to consider power lost from friction, Li et al. (2025) used the following:

$$P_B = \frac{1}{2}B_{\mathrm{m}}\dot{\theta}_{\mathrm{m}}^2 + \frac{1}{2}B_{\mathrm{l}}\dot{\theta}_{\mathrm{l}}^2 + \frac{1}{2}B_{\mathrm{ml}}\left(\dot{\theta}_{\mathrm{m}} + \dot{\theta}_{\mathrm{l}}\right)^2 + \frac{1}{2}B_{\mathrm{sp}}\left(\dot{\theta}_{\mathrm{l}} - \frac{\dot{\theta}_{\mathrm{m}}}{N} + \dot{\tilde{\theta}}_{\mathrm{p}}\right)^2$$

Finally, the scientists utilized the general Lagrange equation for the harmonic drive systems:

$$\begin{cases} \dfrac{\mathrm{d}}{\mathrm{d}t}\left(\dfrac{\partial E}{\partial \dot{\theta}_{\mathrm{m}}}\right) - \dfrac{\partial E}{\partial \theta_{\mathrm{m}}} + \dfrac{\partial V}{\partial \theta_{\mathrm{m}}} + \dfrac{\partial D}{\partial \dot{\theta}_{\mathrm{m}}} = T_{\mathrm{m}} \\ \dfrac{\mathrm{d}}{\mathrm{d}t}\left(\dfrac{\partial E}{\partial \dot{\theta}_{\mathrm{l}}}\right) - \dfrac{\partial E}{\partial \theta_{\mathrm{l}}} + \dfrac{\partial V}{\partial \theta_{\mathrm{l}}} + \dfrac{\partial D}{\partial \dot{\theta}_{\mathrm{l}}} = -T_{\mathrm{l}} \end{cases}$$

Li et al. (2025) synthesized the equations above and utilized Lagrange equations to predict the transmission error for any speed and load without needing to measure most of the specific qualities of each individual testing machine, eventually reaching a formula in:

$$\begin{cases} J_{\mathrm{m}}\ddot{\theta}_{\mathrm{m}} - \left(\dfrac{1}{n} - \dfrac{\mathrm{d}\tilde{\theta}_{\mathrm{p}}}{\mathrm{d}\theta_{\mathrm{m}}}\right)\left[K\left(\theta_l - \dfrac{\theta_{\mathrm{m}}}{n} + \tilde{\theta}_{\mathrm{p}}\right) + B_{\mathrm{sp}}\left(\dot{\theta}_{\mathrm{l}} - \dfrac{\dot{\theta}_{\mathrm{m}}}{n} + \dot{\tilde{\theta}}_{\mathrm{p}}\right)\right] \\ \quad + B_{\mathrm{ml}}\left(\dot{\theta}_{\mathrm{m}} + \dot{\theta}_{\mathrm{l}}\right) + \left(M_2T_{\mathrm{l}} + M_3 + B_{\mathrm{m}}\right)\dot{\theta}_{\mathrm{m}} = T_{\mathrm{m}} \\ \quad J_{\mathrm{l}}\ddot{\theta}_{\mathrm{l}} + K\left(\theta_{\mathrm{l}} - \dfrac{\theta_{\mathrm{m}}}{n} + \tilde{\theta}_{\mathrm{p}}\right) + B_{\mathrm{l}}\dot{\theta}_{\mathrm{l}} + B_{\mathrm{ml}}\left(\dot{\theta}_{\mathrm{m}} + \dot{\theta}_{\mathrm{l}}\right) \\ \quad + B_{\mathrm{sp}}\left(\dot{\theta}_{\mathrm{l}} - \dfrac{\dot{\theta}_{\mathrm{m}}}{n} + \dot{\tilde{\theta}}_{\mathrm{p}}\right) = -M_{\mathrm{l}}T_{\mathrm{l}} - T_{\mathrm{l}} \end{cases}$$

To test how a sudden change in load affects the accuracy of harmonic reduction systems, Li et al. (2025) first started the system with a wave generator speed of 200 rpm with a 40 Nm load. After allowing the system to run for four minutes under these conditions, the researchers dropped the average load to 20 Nm and tracked the apparatus for another 5.2 minutes; they continued this process until they eventually increased the load to 60 Nm. From these changes in load, the scientists discovered that the change in magnitude of load was proportional to the actual change in driving error. A drop from 40 Nm to 20 Nm shifted the baseline position by -3.48 arcmin. Similarly, the error from the 40 Nm to 60 Nm shift creates a similar shift. Changes of load of similar magnitude, the team discovered, led to similar shifts in baseline position. Comparing the actual result to the model's, Li et al. (2025) discovered the simulation result of 3.30 arcmin for a load change of magnitude 20 Nm to be only 0.18 arcmin away from the true result, an error of just 5.17%.

Conclusions

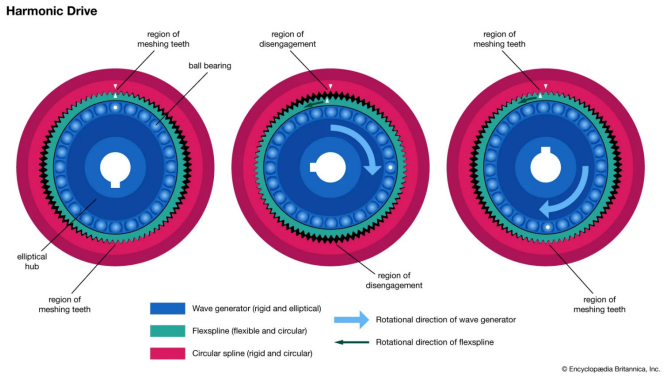
Li et al. (2025) were able to quantify the proportional error of static and dynamic sources using Fourier expansions and Lagrange modeling for each respective category. From their models, they found that dynamic error takes far greater precedence in considering shifts in baseline position than its static counterpart. External changes in load, the scientists determined, were the most limiting factors on a harmonic reducer's accuracy.

To ameliorate the errors they discovered, Li et al. (2025) suggested using stiffer material for a flexspline to lessen the effects of dynamic error due to load changes. Furthermore, since their model was able to relatively accurately assess the error of the system, users of harmonic reducers could write software scripts to adjust according to predicted error.

[^#]: See supplementals on the following page.

Supplementals

[^1] Harmonic drive



Source: Encyclopædia Britannica, Inc. [3].

[^2]

Li et al. used a load of ± 67 Nm because it was the maximum load the harmonic reducer used could withstand without overheating or damage to its elasticity.

[^3]

A Fourier series is a mathematical representation of the sum of repeating sine and cosine waves. Since position from rotational motion over time can be modeled as a wave-like function and all waves are summations of sine and cosine waves, a Fourier transformation is able to quantify a point's motion. The fundamental formula for a trigonometric Fourier expansion is represented by:

$$x(t) = a_0 + \sum_{n=1}^{\infty} (a_n \cos(n\omega_0 t) + b_n \sin(n\omega_0 t))$$

The essential proof for the Fourier Expansion's ability to model a complex wave lies in the fact that all waves are sums of other waves. When two waves collide, they either act in constructive or destructive manners, creating bumps, or reducing or increasing the amplitude of the crests and troughs. So, with enough waves added into the system, as described in the summation of the Fourier Expansion series, one can quantify any wave.

[^3.5]

The order of a Fourier series essentially dictates the number sine and cosine waves added to the overall sum. With a higher order, more sine and cosine waves are used to model the given shape, increasing the accuracy of the model.

[^4]

Funnily enough, the Root Mean Square Error is simply the root of the mean of the squared error. Root Mean Square Error, also called RMSE, represents the average residual error in a model. The closer the end results of the RMSE calculation, the more accurate it is, with zero representing a perfect fit. Though the RMSE method is very helpful in identifying fit when the actual model is similar to the actual value, it is very sensitive to large outliers as the residual error is squared in the calculation:

$$\text{RMSE} = \sqrt{\frac{1}{n}\sum_{i=1}^{n}(y_i - \hat{y}_i)^2}$$

[^5]

The Lagrange equations used in this study serve to combine all known energy in the system (losses and gains) to predict error. [4]

Why Starship?

TED HUANG '29

On September 28, 2026, SpaceX's Starship rocket was successfully launched into a low earth orbit (LEO), an orbit around Earth where the spacecraft usually has an altitude of more than 200km and less than 2000km with an orbital period of less than 128 minutes [1], during its 14th test flight. That day while in orbit, Starship 41 deployed 26 V3 Starlink satellites before reentering the atmosphere. Later, it performed a soft water landing in the Pacific Ocean somewhere north of Hawaii. This test flight marked a major milestone following years of development over the past few years as it was the first time a starship was able to contribute to the payload launches of the starlink program (SpaceX's "connect to wifi from space" project) [2].

Ten years ago, SpaceX had already successfully developed the Falcon 9, a partially reusable launch vehicle fully capable of delivering medium-weight payloads into Low Earth Orbit. Falcon Heavy followed suit, enabling even heavier spacecraft to be launched into different orbits. However, instead of continuing to design the falcon rockets, SpaceX has spent the last few years developing Starship and has spent over $15 billion on this launch vehicle that has not yet been finalized after 14 test flights [3]. Despite these substantial costs, SpaceX continues to work on its design.

One of the reasons is that Starship is designed to provide better payload capacities, and therefore increase efficiency of payload delivery. A standard Falcon 9 launch can deliver approximately 18,500 kg of payload to low earth orbit. In comparison, Starship can deliver up to 100,000 kg to Low Earth Orbit. In terms of starlink satellites, something that SpaceX is launching on a large scale, Starship can launch up to 60 V3 starlink satellites in one launch at maximum configuration, while falcon 9 can only lift at most 30 lighter V2 starlink satellites. Converting this to internet capacity, Starship can provide the internet capacity worth more than 20 falcon 9 launches of Starlink satellites just in one launch [4].

Secondly, Starship is much more cost-effective because it is fully reusable. In recent years, the affordability of sending payload to space has reached unprecedented levels compared to prices before. The space shuttles were the first ever partially reusable launch vehicles targeted at low earth orbit. However, because it had to be manned, it had a cost per kilogram of $54,000 when payload was launched into low earth orbit [5]. Cheaper unmanned rocket models at that time like Atlas (famous for delivering different Mars rovers such as curiosity and perseverance) had a cost of around $10,000 per kilogram to low earth orbit. However, the falcon iteration from SpaceX have both crashed the price of launching to low earth orbit. Falcon 9 for example lowered the cost to approximately $3,000 per kilogram depending on its configuration due to its reusability feature [6]. Reusabilities allow for repetition of launches, thus reducing the total cost. Before falcon came out, expending a booster in an unmanned rocket launch meant you had to build a brand new one. The highest number of times SpaceX has reused a booster was 37 times with booster B1067, while the entire falcon 9 fleet has tallied over 600 reuses in total [7]. Meaning, if the falcon 9 did not have a reusable booster, SpaceX would have built 600 extra falcon 9 boosters to launch these payloads, drastically increasing the price to orbit.

Starship addresses the problem of expensive launch costs by introducing the concept of full reusability. Although falcon class rockets have reusable lower stage boosters, its upper stage is not reusable. Both stages of the starship, however, the Super Heavy lower-stage booster and the Starship upper stage, can and are designed to be caught by the chopsticks, the two arms on the launch tower. Full reusability means nothing has to be replaced or rebuilt after launch, it just has to be refueled. The emergence of Starship turns rockets in the space industry from a single-use craft to a reusable space car. Eventually when Starship enters service, it would be able to achieve a price less than $1,000 per kilogram when launching to low earth orbit and SpaceX plans to bring that number to the two-digit figures in future iterations [8].

Starship holds great significance for the future of spaceflight and rocket design. For example, in the Artemis mission where NASA plans to build a Moon colony, Starship HLS (Human Landing System) is the vessel chosen to land astronauts on the Moon and fly them back into low lunar orbit to re-dock with the mothership Orion [9]. In future missions planned by SpaceX where humans aim to colonize Mars, Starship's reusability will also facilitate the missions by reducing the need for complex reassembling of rockets.



Figure 1. SpaceX's Starship-Super Heavy launch vehicle.

SPACEX, VIA NEXT SPACEFLIGHT [10]

How City Design Shaped the Spread of Disease in Europe and the Pre-Columbian Americas

ALLAN KANG '29

Before Europe's first contact with the Americas in 1492, civilizations of the New World were subjected to small waves of disease and infection from animals in regional environments or localized parasites. However, these ailments were usually centralized in small regions, and there is little evidence of them spreading throughout multiple civilizations. Europe, on the other hand, faced many large pandemics and epidemics such as the Black Death and the Great Plague of London. So what caused these civilizations to encounter diseases in such different manners?

As populations surged throughout the 14th to 16th centuries, infrastructure in cities such as London and Paris can keep packed around a centralized building or plaza to maximize limited space. The limited space for construction and the high population density of many European cities forced the narrowly spaced buildings upwards, further concentrating regions of sewage and waste. Even with improvements in sanitation over following centuries, conditions improved only gradually: even into the early 19th century, most Western cities "had no systematic street cleaning regime," and the carcasses of animals were simply left to rot in the streets [3]. Europeans also lived alongside cattle, pigs, and poultry—the sources from which diseases like measles and influenza are thought to have jumped to humans—whereas the Americas had very few domesticated animals [7]. The inadequate cleaning protocols, combined with the dense narrow streets of cities, concentrated harmful bacteria and pathogens and reduced biodiversity among microbiomes as only certain ones could survive in the stagnant wastes.

The decline in biodiversity favored microorganisms that reproduced quickly, which were typically the ones that carried and spread infectious diseases. This dominance of harmful microorganisms led to a significant increase in the risk of disease exposure to humans and animals [2]. This consequential relationship is conversely modeled in the "dilution effect," a still-debated ecological theory which holds that high biodiversity tends to inhibit the spread of infectious disease [5].

It was a much different case in the isolated Pre-Columbian Americas where population density was generally lower than in Europe. Indigenous people built their cities in areas with ample natural resources such as rivers and jungles. Many Aztec and Mayan city layouts were constructed in precise geometric patterns influenced by the civilization's religion, often including open plazas and spacious roads to support ceremonies and other spiritual events and rituals. Furthermore, unlike European civilizations, many of these American communities built their cities with nature rather than bending it to their will. The Inca Empire, for example, which lived on mountainous terrain, adapted to its surroundings by building temples and other infrastructure around nature, rather than renovating the land.

Due to the differing climates and natural environments, civilizations such as the Aztecs and Inca developed their cities on totally different bases, avoiding many of Europe's problems even where populations were dense. Tenochtitlán, one of the most famous cities in the Americas, had more than 200,000 inhabitants by 1519, more than most European cities, yet it was clean and well planned, with aqueducts bringing in fresh water and a system for collecting trash [1]. Its orderly layout drew on a long tradition of urban planning in central Mexico: at Tula, the earlier Toltec capital that the Aztecs revered, archaeologist Michael E. Smith [6] noted that "large buildings are balanced symmetrically across a square plaza" and that every building follows the same orthogonal grid, creating straight paths and sectors that helped with administration and management. Similarly, the Inca independently developed a different layout, using "kanchas," rectangular and symmetrical walled enclosures adjoined with other similarly designed buildings. Both these examples have ample spacing in their layouts, which made it harder for microorganisms to become concentrated in areas throughout the city. Not only that, the open design and presence of aqueducts allowed plenty of sunlight and water to regularly interact with the land, supporting plant life and healthier soil, which in turn sustained a more diverse and stable microbial environment.

Compared to European designs, the municipal designs of the pre-colonial Americas maintained the balance in biodiversity across the land, disregarding compact streets for a more "unobstructed" design. This balance allowed for a variety of microorganisms to survive, keeping the chance of disease transmission among microbiomes to humans low. Ironically, the same isolation that spared these cities from Old World epidemics would leave their people with no immunity to European disease: when smallpox reached Tenochtitlán in 1520, it killed a large share of the city's population, including its ruler, Cuitláhuac [4].



Detail of Tenochtitlan in the 1524 map.

NEWBERRY LIBRARY/WIKIMEDIA COMMONS, PUBLIC DOMAIN [8]

Why Do We Care About Our Bodies After We Die?

LEO FENG '29

Death is the end of conscious experience—a concept familiar to humanity. From ancient rituals to modern-day pseudoscience, civilization has always been running from the idea of never waking up again. Yet, we often find ourselves caring about our bodies after death. It is paradoxical to care about something posthumously, but our bodies become a symbol of identity even after we die. They provide an image of the people surrounding us, including ourselves. Seeing a dead body makes humans reflect on mortality. It is this fear of dying that pushes us to care about our bodies; by knowing we are in good hands, perhaps we can mitigate that familiar fear.

Psychologists believe in the heavy association between the human body and its thoughts. Terms such as 'body image,' 'schema,' and 'Embodiment of Cognition' have been perpetuated for some years in research. In his book, How the Body Shapes the Mind, Shaun Gallagher writes, "Body image consists of a system of perceptions, attitudes, and beliefs pertaining to one's own body. In contrast, body schema is the system of sensory-motor capacities that function without awareness or the necessity of perceptual monitoring." [1, p. 24] He terms body image as the conscious perception of ourselves while also defining schema as the ability of the body to constantly monitor its own position which is tied to the sensorimotor system. Both terms however, pertain to the association between physical representation and mental abstraction. Gallagher writes about how these terms answer different questions. He writes: "The concept of body image helps to answer the first question about the appearance of the body in the perceptual field; in contrast, the concept of body schema helps to answer the question about how the body shapes the perceptual field." [1, p. 17] Body image is how the body appears to our perception and body schema is how our motor system shapes how we look at ourselves. Gallagher theorizes the inevitable connection between our bodies and perceptions, as both are embodied or associated with physical aspects, the perceptual field [1].

However, Gallagher does not account for how we perceive others with the same phenomena as schema and image. A 2020 article by Coste et al helps reveal a case where body schema and image helps uncover this. Coste investigated how people recognized their own movement without the representation of their bodies. Fifteen participants had their motion mapped with a motion capture suit mapped with seven dots. Participants were asked to distinguish 144 clips that included their own and others as well [2].

As shown in Figure 1, the average unit of change was found to be at 0.71, well above what it should be for chance, meaning that, on average, more people were able to determine their own movement far above than just guessing. Furthermore, they discovered patterns of movement when observing the point light movement diagram. This "kinematic fingerprint" provides certain cues to help patients recognize and distinguish themselves. In other words, the moving dots used in the study contained enough recognizable information for individuality for the patients to see as themselves. This means that it is possible that other people can also recognize you by viewing those dots with enough information on your movement. This aligns with the definition of schema.

Now, how does this relate with death? Even if consciousness is gone, the body still contains what other people associate with you. The body exists even after consciousness ceases and still acts as a carrier of the information that its inhabitant exhibited during the living. A study done by Chapple and Ziebland used 80 participants going through bereavement of loved ones and found that many treated their corpses as if they were still alive. They recognize that it's a corpse, yet they still give the otherwise objective compassion. They were able to recognize their loved ones due to the information that the body still holds post mortem [3].

This proves Gallagher's extensional point. Following Gallagher's idea, if we associate the body to the person, it also conveys to us that they are dead, not living anymore. In this way, a corpse becomes a reminder not only of another person's death but also our own fragility. It changes how we think about our lives and mortality. Now, the body functions as a reminder for the living that their identities are shaped by relationships, values, and social connections that may continue to matter long after death. This phenomenon is called the mortality salience, a state where we become reminded of our own mortality. Because our instincts for survival are built to keep us alive, facing such a primal and instinctive fear would cause anguish and distress. Through a series of studies, researchers Lambert et al investigated this state of being. They found that mortality salience caused increased fear, harmful moods, and fear related language [4].

The fear of death not only shapes how societies respond to dying but also how individuals experience it. Jeff Greenberg, alongside Sheldon Solomon and Tom Pyszczynski, developed Terror Management Theory, suggesting that mortality salience strengthens attachment to cultural values, beliefs, and social identities. Lambert et al, in one of his experiments, observed mortality salience in ingroup favoritism, finding that participants started to favor people that were in their social groups and become more resistant to outsiders. Greenberg and Abram Rosenblatt found that judges who had been reminded of their mortality recommended significantly higher bonds for an accused prostitute than judges who had not received the same reminder. The researchers argued that thoughts of death make people hold more tightly to the values that give their lives meaning [6].

To theorize, this helps explain people's tendency on religious, traditional, and cultural practices when confronted with death or funerals. Ingroup favoritism drives people to revert back to core values—it transforms the concept of death from a frightening unknown into something meaningful and familiar. Through rituals, prayers, and ceremonies, people reaffirm values that help them cope with

the reality of death. Perhaps this is why the treatment of the body matters so much. These rituals and traditions focus on the body. Although the dead can no longer experience what happens to them, caring for the body allows the living to express respect, preserve memory, and reaffirm the beliefs that help them confront mortality.

To answer the question, it is the fear of death that drives us to care about our bodies after we die. Bodies remain a representation of a person post mortem and inadvertently causing stress. Death requires us to face what cannot be avoided, explained away, or escaped. Funerals and other rituals become ways in which people cope with mortality. It offers the promise that our lives will mean something even after we are gone. Death becomes easier to face when we know that we will be remembered, respected, and loved. Perhaps, this theory may explain why the prospect of dying without dignity or remembrance is so frightening. The body remains a symbol of identity, memory, and the values that connect us to one another. In caring for the dead, we find a way to cope with death itself.

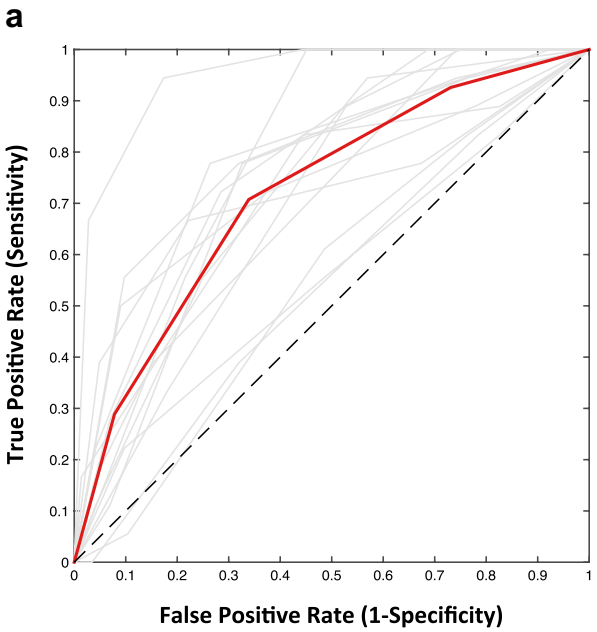


Figure 1. Self-recognition from movement. Gray curves show individual participants' performance; the red curve shows the average. The dashed diagonal marks chance performance. Mean area under the curve was 0.71.

COSTE ET AL. (2021), FIG. 3A (CROPPED); CC BY 4.0 [2]

Citations

A New Look Into the Past: The Newest NASA Telescope, Nancy Grace Roman

[1] American Association of University Women. (2020, September 30). *Nancy Grace Roman: The life and legacy of a NASA star*. https://www.aauw.org/resources/faces-of-aauw/nancy-grace-roman-the-life-and-legacy-of-a-nasa-star/

[2] Canadian Space Agency. (2026, August 31). *Nancy Grace Roman Space Telescope: Uncovering the mysteries of dark matter, dark energy and exoplanets*. https://www.asc-csa.gc.ca/eng/satellites/nancy-grace-roman/

[3] Cull, M. (2026, June 12). *NASA's Nancy Grace Roman Space Telescope's 'spy mirror' could transform how we map the universe*. Discover Magazine. https://www.discovermagazine.com/nasa-s-nancy-grace-roman-space-telescope-s-spy-mirror-could-transform-how-we-map-the-universe-49239

[4] Gohd, C. (2026, August 26). *From spy satellite to space telescope: The unlikely origins of NASA's Roman Space Telescope*. Space.com. https://www.space.com/astronomy/from-spy-satellite-to-space-telescope-the-unlikely-origins-of-nasas-roman-space-telescope

[5] Krebs, G. D. (2026, August 31). *NGRST (Nancy Grace Roman Space Telescope, WFIRST)*. Gunter's Space Page. https://space.skyrocket.de/doc_sdat/wfirst.htm

[6] L3Harris Technologies. (2026, August 30). *L3Harris celebrates successful launch of NASA's Nancy Grace Roman Space Telescope* [Press release]. https://www.l3harris.com/newsroom/press-release/2026/08/l3harris-celebrates-successful-launch-nasas-nancy-grace-roman-space

[7] Lambier, S. (2026, September 29). *How NASA's Nancy Grace Roman Space Telescope will open a window into the Milky Way*. Phys.org. https://phys.org/news/2026-09-nasa-nancy-grace-roman-space.html

[8] Lerner, L. (2024, September 16). *Dark energy, explained*. University of Chicago News. https://news.uchicago.edu/explainer/dark-energy-explained

[9] Malayil, J. (2026, August 31). *NASA launches new telescope that can scan the universe 1,000 times faster than Hubble*. Interesting Engineering. https://interestingengineering.com/space/nasa-launches-new-telescope-that-can-scan-the-universe-1000-times-faster-than-hubble

[10] Museum of Science. (2026, June 6). *Ready for Roman: The Nancy Grace Roman Space Telescope*. https://www.mos.org/article/ready-roman-nancy-grace-roman-space-telescope

[11] Space Telescope Science Institute. (n.d.). *Nancy Grace Roman Space Telescope*. Retrieved October 10, 2026, from https://www.stsci.edu/roman

[12] Space Telescope Science Institute. (2026, July 14). *NASA's Roman telescope will spot distant black holes that shred stars* [Press release]. https://www.stsci.edu/contents/news-releases/2026/news-2026-203

[13] Stahl, A. (2026, August 30). *The Nancy Grace Roman Space Telescope has launched*. The Planetary Society. https://www.planetary.org/articles/the-nancy-grace-roman-space-telescope-launch

[14] Szőcs, T. (2009, September 15). *Cassegrain telescope* [Illustration]. Wikimedia Commons. https://commons.wikimedia.org/wiki/File:Cassegrain.en.png. CC BY-SA 3.0. https://creativecommons.org/licenses/by-sa/3.0/

[15] NASA's Goddard Space Flight Center. (n.d.). *Artist's illustration of the Nancy Grace Roman Space Telescope* [Illustration]. Museum of Science. https://www.mos.org/article/ready-roman-nancy-grace-roman-space-telescope

[16] Kraus, J. (2026, August 30). *Falcon Heavy carrying NASA's Roman telescope launches from Kennedy Space Center in Florida* [Photograph]. Interesting Engineering. https://interestingengineering.com/space/nasa-launches-new-telescope-that-can-scan-the-universe-1000-times-faster-than-hubble

Are Boltzmann Brains Real?

[1] Balibrea, F. (2016). On Clausius, Boltzmann and Shannon notions of entropy. *Journal of Modern Physics, 7*(2), 219–227. https://doi.org/10.4236/jmp.2016.72022

[2] Boddy, K. K., & Carroll, S. M. (2013). *Can the Higgs boson save us from the menace of the Boltzmann brains?*. arXiv. https://doi.org/10.48550/arXiv.1308.4686

[3] Carroll, S. M. (2017). *Why Boltzmann brains are bad*. arXiv. https://doi.org/10.48550/arXiv.1702.00850

[4] CMS Collaboration. (2023). Measurement of the top quark pole mass using top quark–antiquark + jet events in the dilepton final state in proton-proton collisions at $\sqrt{s}$ = 13 TeV. *Journal of High Energy Physics, 2023*(7), Article 77. https://doi.org/10.1007/JHEP07(2023)077

[5] Thomson, W. (1862, March 5). On the age of the sun's heat. *Macmillan's Magazine, 5*, 388–393.

[6] Day, S. (2024). *A close up of a human brain on a black background* [Photograph]. Unsplash. https://unsplash.com/photos/a-close-up-of-a-human-brain-on-a-black-background-ii6BOPjAtVY
[7] *Ludwig Boltzmann* [Photograph]. (1902). Wikimedia Commons. https://commons.wikimedia.org/wiki/File:Boltzmann-Ludwig.jpg
[8] New World Encyclopedia. (n.d.). *Standard Model of Elementary Particles [Diagram]. In Fermion*. https://www.newworldencyclopedia.org/entry/Fermion

Effectiveness and Safety of rVSV-ZEBOV Vaccine Against Zaire Ebola Virus

[1] World Health Organization. (n.d.). *Ebola disease*. https://www.who.int/health-topics/ebola
[2] Centers for Disease Control and Prevention. (2024, May 15). *Ebola disease basics*. https://www.cdc.gov/ebola/about/index.html
[3] World Health Organization. (n.d.). *Ebola outbreak 2014–2016 - West Africa*. https://www.who.int/emergencies/situations/ebola-outbreak-2014-2016-West-Africa
[4] World Health Organization. (n.d.). *Ebola virus disease vaccines*. https://www.who.int/teams/regulation-prequalification/eul/ebola-vaccines
[5] World Health Organization Ebola Response Team. (2016). After Ebola in West Africa — Unpredictable risks, preventable epidemics. *New England Journal of Medicine, 375*(6), 587–596. https://doi.org/10.1056/NEJMsr1513109
[6] European Medicines Agency. (2025, January 24). *Ervebo*. https://www.ema.europa.eu/en/medicines/human/EPAR/ervebo
[7] Halperin, S. A., Das, R., Onorato, M. T., Liu, K., Martin, J., Grant-Klein, R. J., Nichols, R., Coller, B. A., Helmond, F. A., Simon, J. K., & V920-012 Study Team. (2019). Immunogenicity, lot consistency, and extended safety of rVSVΔG-ZEBOV-GP vaccine: A phase 3 randomized, double-blind, placebo-controlled study in healthy adults. *The Journal of Infectious Diseases, 220*(7), 1127–1135. https://doi.org/10.1093/infdis/jiz241
[8] Alabi, A., Kokou, K., Mahmoudou, S., Kavishna, R., Nakka, S. S., Rothenberger, S., Musangomunei, F. P., Olubiyi, B. F., Bie-Ondo, J. C., Kabwende, A. L., Velavan, T. P., VSV-EBOPLUS Consortium, Medaglini, D., Nakaya, H. I., Engler, O., Harandi, A. M., Siegrist, C. A., Kremsner, P. G., & Agnandji, S. T. (2024). Replication, safety and immunogenicity of the vectored Ebola vaccine rVSV-ΔG-ZEBOV-GP in a sub-Saharan African paediatric population: A randomised controlled, open-label trial in children aged 1–12 years living in Lambaréné, Gabon. *Journal of Infection, 89*(4), Article 106237. https://doi.org/10.1016/j.jinf.2024.106237
[9] Watson, C. H., Gsell, P. S., Hall, Y., Camacho, A., Riveros, X., Enwere, G., Vicari, A., Nadlaou, S. D., Toure, A., Sani, I. M., Diallo, A., Kolie, C., Duraffour, S., Ifono, K., Maomou, A., Dore, K., Djidonou, H. A., Bagayoko, A., Damey, P. P., . . . Henao-Restrepo, A. M. (2024). rVSV-ZEBOV vaccination in people with pre-existing immunity to Ebolavirus: An open-label safety and immunogenicity study in Guinean communities affected by Ebola virus disease (l'essai proches). *BMC Medicine, 22*(1), Article 523. https://doi.org/10.1186/s12916-024-03726-z
[10] Davey, R. T., Jr., Collins, G. L., Rouphael, N., Poliquin, G., McConnell, R., Grubbs, G., Moir, S. L., Langley, J. M., Teitelbaum, M., Hewlett, A. L., McLellan, S. L. F., Bhadelia, N., Raabe, V. N., Mulligan, M. J., Maljkovic Berry, I., Dighero-Kemp, B., Kurtz, J. R., Hensley, L. E., Dozier, N. C. E., . . . Neaton, J. D. (2024). Safety and immunogenicity of a delayed booster dose of the rVSVΔG-ZEBOV-GP vaccine for prevention of Ebola virus disease: A multicentre, open-label, phase 2 randomised controlled trial. *The Lancet Microbe, 5*(11), Article 100923. https://doi.org/10.1016/S2666-5247(24)00163-0
[11] Juan-Giner, A., Tchaton, M., Jemmy, J. P., Soumah, A., Boum, Y., Faga, E. M., Cisse, M., & Grais, R. F. (2019). Safety of the rVSV ZEBOV vaccine against Ebola Zaire among frontline workers in Guinea. *Vaccine, 37*(48), 7171–7177. https://doi.org/10.1016/j.vaccine.2018.09.009
[12] Davis, C., Tipton, T., Sabir, S., Aitken, C., Bennett, S., Becker, S., Evans, T., Fehling, S. K., Gunson, R., Hall, Y., Jackson, C., Johanssen, I., Kieny, M. P., Mcmenamin, J., Spence, E., Strecker, T., Sykes, C., Templeton, K., Thorburn, F., . . . Thomson, E. C. (2020). Postexposure prophylaxis with rVSV-ZEBOV following exposure to a patient with Ebola virus disease relapse in the United Kingdom: An operational, safety, and immunogenicity report. *Clinical Infectious Diseases, 71*(11), 2872–2879. https://doi.org/10.1093/cid/ciz1165
[13] Diallo, A., Carlos-Bolumbu, M., Cervantes-Gonzalez, M., Wozniak, V., Diallo, M. H., Diallo, B. D., Delamou, A., & Galtier, F. (2021). Immunogenicity and safety of Ebola virus vaccines in healthy adults: A systematic review and network meta-analysis. *Human Vaccines & Immunotherapeutics, 17*(10), 3771–3783. https://doi.org/10.1080/21645515.2021.1932214
[14] Legardy-Williams, J. K., Carter, R. J., Goldstein, S. T., Jarrett, O. D., Szefer, E., Fombah, A. E., Tinker, S. C., Samai, M., & Mahon, B. E. (2020). Pregnancy outcomes among women receiving rVSVΔ-ZEBOV-GP Ebola vaccine during the Sierra Leone Trial to Introduce a Vaccine against Ebola. *Emerging Infectious Diseases, 26*(3), 541–548. https://doi.org/10.3201/eid2603.191018
[15] Goldsmith, C. (n.d.). *Ebola virus virion [Colorized transmission electron micrograph]. CDC, Public Health Image Library, image 10816. Public domain*. https://commons.wikimedia.org/wiki/File:Ebola_virus_virion.jpg

Exoplanets: A World Outside of Our Own

[1] NASA. (n.d.). *Exoplanets*. Retrieved October 25, 2026, from https://science.nasa.gov/exoplanets/
[2] The Schools' Observatory. (n.d.). *The first discoveries*. https://www.schoolsobservatory.org/learn/space/exoplanets/history
[3] Armitage, P. J. (2024). *Planet formation theory: An overview* [Preprint]. arXiv. https://doi.org/10.48550/arXiv.2412.11064
[4] NASA. (2024, October 29). *Terrestrial*. https://science.nasa.gov/exoplanets/terrestrial/

[5] NASA. (2024, October 28). *What is a super-Earth?* https://science.nasa.gov/exoplanets/super-earth/

[6] Lakdawalla, E. (2020, March 2). *The different kinds of exoplanets you meet in the Milky Way*. The Planetary Society. https://www.planetary.org/articles/the-different-kinds-of-exoplanets-you-meet-in-the-milky-way

[7] European Space Agency. (n.d.). *How to find an exoplanet*. https://www.esa.int/Science_Exploration/Space_Science/Exoplanets/How_to_find_an_exoplanet

[8] NASA, European Space Agency, Canadian Space Agency, & Player, D. (2021, November 17). *Diagram of an exoplanet phase curve* [Illustration]. NASA Science. https://science.nasa.gov/asset/webb/diagram-of-an-exoplanet-phase-curve/

The Types of Prion Diseases

[1] Holman, A. P., & Kurouski, D. (2025). Prion diseases: Lessons from historical outbreaks and potential emerging ones. *Protein Science*, *34*(6), Article e70175. https://doi.org/10.1002/pro.70175

[2] Centers for Disease Control and Prevention. (2026, February 20). *About prion diseases*. https://www.cdc.gov/prions/about/index.html

[3] National Institute of Neurological Disorders and Stroke. (n.d.). *Creutzfeldt-Jakob disease*. National Institutes of Health. https://www.ninds.nih.gov/sites/default/files/2025-05/creutzfeldt-jakob-disease.pdf

[4] Centers for Disease Control and Prevention. (2024, November 12). *Clinical overview of variant Creutzfeldt-Jakob disease*. https://www.cdc.gov/variant-creutzfeldt-jakob/hcp/clinical-overview/index.html

[5] Centers for Disease Control and Prevention. (2025, December 9). *Bovine spongiform encephalopathy (BSE)*. https://www.cdc.gov/mad-cow/php/animal-health/index.html

[6] Cleveland Clinic. (2023, April 28). *Fatal familial insomnia*. https://my.clevelandclinic.org/health/diseases/25001-fatal-familial-insomnia

[7] Gibson, L. (2026, August 10). Harvard couple aim to cure prion diseases. *Harvard Magazine*. https://www.harvardmagazine.com/research/harvard-prion-disease-sonia-vallabh-eric-minikel

[8] Jenny, A. (2003). *Brain tissue affected by bovine spongiform encephalopathy (BSE)* [Photomicrograph; PHIL ID 5435]. Centers for Disease Control and Prevention, Public Health Image Library. https://wwwn.cdc.gov/phil/Details.aspx?pid=5435

An Overview of CRISPR

[1] Deltcheva, E., Chylinski, K., Sharma, C. M., Gonzales, K., Chao, Y., Pirzada, Z. A., Eckert, M. R., Vogel, J., & Charpentier, E. (2011). CRISPR RNA maturation by trans-encoded small RNA and host factor RNase III. *Nature*, *471*(7340), 602–607. https://doi.org/10.1038/nature09886

[2] Jinek, M., Chylinski, K., Fonfara, I., Hauer, M., Doudna, J. A., & Charpentier, E. (2012). A programmable dual-RNA-guided DNA endonuclease in adaptive bacterial immunity. *Science*, *337*(6096), 816–821. https://doi.org/10.1126/science.1225829

[3] Tisch, M. (n.d.). *CRISPR Cas9* [Illustration]. Bioicons. https://bioicons.com/icons/cc-0/Genetics/Marcel_Tisch/CRISPR_Cas9.svg

Origin of Life: Spontaneous Proliferation?

[1] Koppes, S. (2022, September 12). *The origin of life on Earth, explained*. University of Chicago News. https://news.uchicago.edu/explainer/origin-life-earth-explained

[2] Mandal, P., & Abramson, J. (n.d.). *Primordial soup theory & model*. Study.com. https://study.com/learn/lesson/primordial-soup-theory-model.html

[3] Scoville, H. (2018, March 5). *Early life theories: Primordial soup*. ThoughtCo. https://www.thoughtco.com/early-life-theory-of-primordial-soup-1224531

[4] Scoville, H. (2018, January 23). *Early life theories: Hydrothermal vents*. ThoughtCo. https://www.thoughtco.com/early-life-theory-of-hydrothermal-vents-1224529

[5] Scharping, N. (2021, May 10). *Did life on Earth come from outer space?*. Astronomy. https://www.astronomy.com/science/did-life-on-earth-come-from-outer-space/

[6] Explore Yeast. (2022, May 13). *Louis Pasteur: The father of fermentation*. https://www.exploreyeast.com/yeast-and-fermentation/louis-pasteur-the-father-of-fermentation/

[7] Bailey, R. (2019, October 23). *Is spontaneous generation real?*. ThoughtCo. https://www.thoughtco.com/spontaneous-generation-4118145

[8] Edelfelt, A. (1885). *Louis Pasteur* [Painting]. Wikimedia Commons. https://en.wikipedia.org/wiki/File:Albert_Edelfelt_-_Louis_Pasteur_-_1885.jpg

[9] Miller, W. (1955, May 2). Old man's advice to youth: "Never lose a holy curiosity." *Life, 38*(18), 62–64. https://books.google.com/books?id=dlYEAAAAMBAJ

HistGramBench: Can AI Pass Mr. Dollhopf's Geometry Class?

[1] Belouadi, J., Ponzetto, S. P., & Eger, S. (2024). *DeTikZify: Synthesizing graphics programs for scientific figures and sketches with TikZ*. arXiv. https://doi.org/10.48550/arXiv.2405.15306

[2] Benjamini, Y., & Hochberg, Y. (1995). Controlling the false discovery rate: A practical and powerful approach to multiple testing. *Journal of the Royal Statistical Society: Series B (Methodological), 57*(1), 289–300. https://doi.org/10.1111/j.2517-6161.1995.tb02031.x

[3] Ibragimov, R., & Müller, U. K. (2010). t-statistic based correlation and heterogeneity robust inference. *Journal of Business & Economic Statistics, 28*(4), 453–468. https://doi.org/10.1198/jbes.2009.08046

[4] Levchenko, M. (2025). *Evaluating LLMs for historical document OCR: A methodological framework for digital humanities*. arXiv. https://doi.org/10.48550/arXiv.2510.06743

[5] Lu, P., Bansal, H., Xia, T., Liu, J., Li, C., Hajishirzi, H., Cheng, H., Chang, K.-W., Galley, M., & Gao, J. (2023). *MathVista: Evaluating mathematical reasoning of foundation models in visual contexts*. arXiv. https://doi.org/10.48550/arXiv.2310.02255

[6] Lu, P., Gong, R., Jiang, S., Qiu, L., Huang, S., Liang, X., & Zhu, S.-C. (2021). *Inter-GPS: Interpretable geometry problem solving with formal language and symbolic reasoning*. arXiv. https://doi.org/10.48550/arXiv.2105.04165

[7] Si, C., Zhang, Y., Li, R., Yang, Z., Liu, R., & Yang, D. (2024). *Design2Code: Benchmarking multimodal code generation for automated front-end engineering*. arXiv. https://doi.org/10.48550/arXiv.2403.03163

[8] Wu, C., Ge, Y., Guo, Q., Wang, J., Liang, Z., Lu, Z., Shan, Y., & Luo, P. (2024). *Plot2Code: A comprehensive benchmark for evaluating multi-modal large language models in code generation from scientific plots*. arXiv. https://doi.org/10.48550/arXiv.2405.07990

[9] Zheng, L., Chiang, W.-L., Sheng, Y., Zhuang, S., Wu, Z., Zhuang, Y., Lin, Z., Li, Z., Li, D., Xing, E. P., Zhang, H., Gonzalez, J. E., & Stoica, I. (2023). *Judging LLM-as-a-judge with MT-Bench and Chatbot Arena*. arXiv. https://doi.org/10.48550/arXiv.2306.05685

[10] Tran, H. (n.d.). *HistGramBench: Can AI pass Mr. Dollhopf's geometry class?*. Deerfield Academy. Figure 1 reproduces historical diagrams identified in the figure; Figures 2–5 and Tables 1–3 present the author's benchmark design and results.

Bacteria as Living Circuit Boards

[1] Trafton, A. (2026, August 17). *MIT engineers connect bacteria to create living transistors*. MIT News. https://news.mit.edu/2026/mit-engineers-connect-bacteria-to-create-living-transistors-0817

[2] Puiu, T. (2026, August 19). *Scientists turn bacteria into transistors to build living circuit boards*. ZME Science. https://www.zmescience.com/science/news-science/scientists-turn-bacteria-into-transistors-to-build-living-circuit-boards/

[3] Doosthosseini, H., Chen, H., & Voigt, C. A. (2026). Living circuit boards built by printing bacterial transistors. *Nature Chemical Biology*. Advance online publication. https://doi.org/10.1038/s41589-026-02300-3

[4] Loughran, J. (2026, August 18). *Living bacteria used to build complex computing circuits by MIT team*. Engineering & Technology. https://eandt.theiet.org/2026/08/18/living-bacteria-used-build-complex-computing-circuits-mit-team

[5] Gahan, C. G., Van Lehn, R. C., Blackwell, H. E., & Lynn, D. M. (2021). Interactions of bacterial quorum sensing signals with model lipid membranes: Influence of acyl tail structure on multiscale response. *Langmuir, 37*(41), 12049–12058. https://doi.org/10.1021/acs.langmuir.1c01825

[6] Churchill, M. E. A., & Chen, L. (2011). Structural basis of acyl-homoserine lactone-dependent signaling. *Chemical Reviews, 111*(1), 68–85. https://doi.org/10.1021/cr1000817

[7] Massachusetts Institute of Technology. (2026, September 4). *MIT turns bacteria into living transistors*. ScienceDaily. https://www.sciencedaily.com/releases/2026/09/260901070526.htm

[8] *Living circuit boards made from engineered bacterial colonies* [Image]. (2026). MIT News. https://news.mit.edu/2026/mit-engineers-connect-bacteria-to-create-living-transistors-0817. Courtesy of the researchers, edited by MIT News. CC BY-NC-ND 3.0. https://creativecommons.org/licenses/by-nc-nd/3.0/

Quantifying Error in Harmonic Reduction Systems

[1] Harmonic Drive LLC. (2021). Harmonic drive® strain wave gear - zero backlash. https://staging.harmonicdrive.net/technology

[2] Li, R., Zhou, G., Zhao, Z., Li, J., & Wang, J. (2025). Analysis and prediction of transmission error of harmonic reducer for space robot. Space: Science & Technology, 5, Article 0233. https://doi.org/10.34133/space.0233. CC BY 4.0. https://creativecommons.org/licenses/by/4.0/

[3] Britannica Editors. (2022, January 7). Harmonic Drive. Encyclopædia Britannica. https://www.britannica.com/technology/Harmonic-Drive

[4] Lecture L20 - Energy methods: Lagrange's equations. (n.d.). MIT OpenCourseWare. Retrieved October 12, 2026, from https://ocw.mit.edu/courses/16-07-dynamics-fall-2009/b39e882f1524a0f6a98553ee33ea6f35_MIT16_07F09_Lec20.pdf

Why Starship?

[1] Federal Aviation Administration. (2025, May 2). *Frequently asked questions (FAQs)*. https://www.faa.gov/space/additional_information/faq#s1

[2] Weber, R. (n.d.). *Ship 41 makes it to orbit, Booster 21 nearly perfect*. NASASpaceflight. https://www.nasaspaceflight.com/2026/09/starship-flight-14-orbit/

[3] Roulette, J., & Wang, E. (2026, May 1). *SpaceX spending on Starship tops $15 billion in rush for airline-like rocketry*. Reuters. https://www.reuters.com/business/autos-transportation/spacex-spending-starship-tops-15-billion-rush-airline-like-rocketry-2026-05-01/

[4] Merritt, S. [@SawyerMerritt]. (2026, June 10). [Comparison of Starlink capacity on Starship and Falcon 9] [Post]. X. https://x.com/SawyerMerritt/status/2064567710751601040

[5] Orbital Radar. (n.d.). *How much does it cost to launch a rocket?* Retrieved October 25, 2026, from https://orbitalradar.com/space-economy/launch-cost-trends

[6] Wang, B. (2025, January 20). *SpaceX Starship roadmap lower launch costs by 100 times*. NextBigFuture. https://www.nextbigfuture.com/2025/01/spacex-starship-roadmap-to-100-times-lower-cost-launch.html

[7] SpaceX. (n.d.). *Falcon 9*. Retrieved October 25, 2026, from https://www.spacex.com/vehicles/falcon-9

[8] Zafar, R. (2020, November 18). *Elon Musk reiterates insanely low Starship launch costs of $10/kg*. Wccftech. https://wccftech.com/elon-musk-starship-launch-cost-reiterate/

[9] Orbital Radar. (2026, September 13). *Starship HLS*. https://orbitalradar.com/spacecraft/starship-hls

[10] Next Spaceflight. (n.d.). *Starlink Group 31-1*. Retrieved October 25, 2026, from https://nextspaceflight.com/launches/details/8346/

How City Design Shaped the Spread of Disease in Europe and the Pre-Columbian Americas

[1] Barr, S. (n.d.). *Early American civilizations: The Aztec and Inca. In United States history I*. Lumen Learning. https://courses.lumenlearning.com/wm-ushistory1/chapter/early-american-civilizations-the-aztec-and-inca/

[2] Cary Institute of Ecosystem Studies. (2020, April 29). *The more we lose biodiversity, the worse will be the spread of infectious diseases*. https://www.caryinstitute.org/news-insights/media-coverage/more-we-lose-biodiversity-worse-will-be-spread-infectious-diseases

[3] European Cleaning Journal. (2013, May 15). *Cleaning towns and streets – a history*. https://www.europeancleaningjournal.com/magazine/articles/latest-news/cleaning-towns-and-streets-a-history

[4] McCaa, R. (1995). Spanish and Nahuatl views on smallpox and demographic catastrophe in the conquest of Mexico. *Journal of Interdisciplinary History, 25*(3), 397–431.

[5] McCallum, H. I. (2015). Lose biodiversity, gain disease. *Proceedings of the National Academy of Sciences, 112*(28), 8523–8524. https://doi.org/10.1073/pnas.1510607112

[6] Smith, M. E. (2011, October 24). *Urban planning in ancient Central Mexico*. Wide Urban World. https://wideurbanworld.blogspot.com/2011/10/urban-planning-in-ancient-central.html

[7] Wolfe, N. D., Dunavan, C. P., & Diamond, J. (2007). Origins of major human infectious diseases. *Nature, 447*(7142), 279–283. https://doi.org/10.1038/nature05775

[8] *Map of Tenochtitlan and the Gulf of Mexico* [Map]. (1524). Newberry Library. Wikimedia Commons. https://commons.wikimedia.org/wiki/File:Map_of_Tenochtitlan_and_Gulf_of_Mexico,_1524.jpg. Public domain.

Why do we care about our bodies after we die?

[1] Gallagher, S. (2005). *How the body shapes the mind*. Clarendon Press. https://doi.org/10.1093/0199271941.001.0001

[2] Coste, A., Bardy, B. G., Janaqi, S., Słowiński, P., Tsaneva-Atanasova, K., Goupil, J. L., & Marin, L. (2021). Decoding identity from motion: How motor similarities colour our perception of self and others. *Psychological Research*, *85*(2), 509–519. https://doi.org/10.1007/s00426-020-01290-8

[3] Chapple, A., & Ziebland, S. (2010). Viewing the body after bereavement due to a traumatic death: Qualitative study in the UK. *BMJ*, *340*, Article c2032. https://doi.org/10.1136/bmj.c2032

[4] Lambert, A. J., Eadeh, F. R., Peak, S. A., Scherer, L. D., Schott, J. P., & Slochower, J. M. (2014). Toward a greater understanding of the emotional dynamics of the mortality salience manipulation: Revisiting the "affect-free" claim of terror management research. *Journal of Personality and Social Psychology*, *106*(5), 655–678. https://doi.org/10.1037/a0036353

[5] Greenberg, J., Koole, S. L., & Pyszczynski, T. (Eds.). (2013). *Handbook of experimental existential psychology*. Guilford Press.

[6] Rosenblatt, A., Greenberg, J., Solomon, S., Pyszczynski, T., & Lyon, D. (1989). Evidence for terror management theory: I. The effects of mortality salience on reactions to those who violate or uphold cultural values. *Journal of Personality and Social Psychology*, *57*(4), 681–690. https://doi.org/10.1037/0022-3514.57.4.681

Credits

Faculty Advisor	Mark Acton
Co-Editors-in-Chief	Torge Blunck ’27 Yong Ding ’27
Co-Managing Editors	Ellie Maeda ’27 Alice Chen ’28 Carter He ’28
Editorial Board	Jerry Du ’27 Gabby Kilroy ’29 Julia Lu ’28 Harry Tran ’28 Krystal Zhang ’29
Photography Editor	Thijs Wittink ’27

DEERFIELD ACADEMY

Focal Point Magazine

November 2026 • Volume X • Issue 2

7 Boyden Lane, Deerfield, MA 01342, United States of America